ELSEVIER

Biochimica et Biophysica Acta 1462 (1999) 157–183

BIOCHIMICA ET BIOPHYSICA ACTA
BBA

www.elsevier.com/locate/bba

Review

The structure, dynamics and orientation of antimicrobial peptides in membranes by multidimensional solid-state NMR spectroscopy

Burkhard Bechinger *

Max Planck Institute for Biochemistry, Am Klopferspitz 18A, 82152 Martinsried, Germany

Accepted 5 October 1999

Abstract

Linear peptide antibiotics have been isolated from amphibians, insects and humans and used as templates to design cheaper and more potent analogues for medical applications. Peptides such as cecropins or magainins are ≤40 amino acids in length. Many of them have been prepared by solid-phase peptide synthesis with isotopic labels incorporated at selected sites. Structural analysis by solid-state NMR spectroscopy and other biophysical techniques indicates that these peptide antibiotics strongly interact with lipid membranes. In bilayer environments they exhibit amphipathic α-helical conformations and alignments of the helix axis parallel to the membrane surface. This contrasts the transmembrane orientations observed for alamethicin or gramicidin A. Models that have been proposed to explain the antibiotic and pore-forming activities of membrane-associated peptides, as well as other experimental results, include transmembrane helical bundles, wormholes, carpets, detergent-like effects or the in-plane diffusion of peptide-induced bilayer instabilities.

Keywords: Amphipathic peptide; Polypeptide–lipid interaction; Peptide pore formation; Phospholipid membrane; Regulation; Selectivity; Cecropin; Magainin; Melittin; Alamethicin; Gramicidin A; Dermaseptin

Contents

Abbreviations: ATR, attenuated total reflection; CD, circular dichroism; DMPC, 1,2-dimyristoyl-*sn*-glycero-3-phosphocholine; DMPG, 1,2-dimyristoyl-*sn*-glycero-3-phosphoglycerol; DMPS, 1,2-dimyristoyl-*sn*-glycero-3-phosphoserine; DOPA, 1,2-dioleoyl-*sn*-glycero-3-phosphatidic acid; DPC, dodecyl phosphocholine; DPPC, 1,2-dipalmitoyl-*sn*-glycero-3-phosphocholine; DPPG, 1,2-dipalmitoyl-*sn*-glycero-3-phosphoglycerol; DSPC, 1,2-distearoyl-*sn*-glycero-3-phosphocholine; ESR, electron spin resonance; FTIR, Fourier transform infrared; IR, infrared; MAS, magic angle spinning; M_r, molecular mass; NMR, nuclear magnetic resonance; NOE, nuclear Overhauser enhancement; PC, 1-2-diacyl-*sn*-glycero-3-phosphocholine; PE, 1,2-diacyl-*sn*-glycerol-3-phosphoethanolamine; PG, 1,2-diacyl-*sn*-glycerol-3-phosphoglycerol; POPC, 1-palmitoyl-2-oleoyl-*sn*-glycero-3-phosphocholine; POPE, 1-palmitoyl-2-oleoyl-*sn*-glycero-3-phosphoethanolamine; POPG, 1-palmitoyl-2-oleoyl-*sn*-glycero-3-phosphoglycerol; PS, 1,2-diacyl-*sn*-glycerol-3-phosphoserine; REDOR, rotational-echo double-resonance; SDS, sodium dodecyl sulfate; TFE, trifluoroethanol

* Fax: +49 89 8578-2876; E-mail: bechinge@biochem.mpg.de

0005-2736/99/$ – see front matter
PII: S0005-2736(99)00205-9

1. Introduction

The widespread increase in resistance of bacteria and fungi against many of the commonly used antibiotics has raised interest in the discovery and development of new compounds that yield efficient protection when infections occur. Fortunately, peptide antibiotics are found in many species including amphibians, insects or humans, and the discovery of new active compounds has often been a result of the investigation of nature's gifts [1–5]. Analysis of these compounds indicates that a large variety of hydrophobic and amphipathic peptide antibiotics are synthesised, stored and secreted in considerable quantities. The availability of these substances establishes a defence system that can be set into action immediately when infections occur. Understanding the structure–function relationship of these peptides allows for the design of cheaper and more efficient analogues [6,7]. The systems of particular interest for pharmacological applications are those which exhibit immunological or tumoricidal activity, but, under the same experimental conditions, do not show haemolytic or cytotoxic activity against healthy vertebrate cells.

The scope of this article is to review some of the structural studies, with emphasis on solid-state NMR experiments, applied to membrane-active peptides. In order to correlate the structural and functional characteristics of these peptides, however, discussion of results obtained by other techniques is essential. A common characteristic observed for membrane-active peptides is their capability to disturb bilayer integrity, either by disruption or pore formation. The resulting openings in the lipid bilayer lead to the collapse of the transmembrane electrochemical gradients and, therefore, can explain the cell-killing activities of these peptides (reviewed, e.g., in [5,6, 8–10]). The formation of pores deprives sensitive organisms of their source of energy and results in increased water and ion flow across the membrane concomitant with cell swelling and osmolysis [11,12]. A detailed understanding of the mechanisms of channel formation and cell lysis will allow for the rationale design of new antibiotics in the future.

The availability of efficient analytical and preparative techniques has allowed the application of many biophysical methods for the study of these peptides (reviewed in [6,7]). These include X-ray crystallography, NMR spectroscopy in solution and in the presence of lipid bilayers, as well as FTIR, Raman, fluorescence and CD optical spectroscopies. Solid-phase peptide synthesis is a versatile technique that allows one to obtain high yields of peptide [13,14]. The combination of solid-state NMR spectroscopy and chemical methods has proven particularly powerful, as the latter allow for the incorporation of isotopic labels at single sites as well as modifications of the peptide sequence almost at will.

Many of the membrane-active peptide antibiotics have been synthesised and purified by chemical or biochemical methods in quantities sufficient for conformational and functional analyses. Although structural studies at high resolution are prerequisites to understanding the functional mechanisms of membrane-active peptides, it should be kept in mind that structural methods provide a view of the peptide–lipid macromolecular complexes in their low-energy equilibrium states. The functional properties observed may, however, be the result of a minor population of the peptide in rarely-occurring higher energy configurations. It is, therefore, the critical assessment of both structural and functional studies that will ultimately allow one to understand the functional mechanisms of these peptides.

The detailed chemical environment exhibits a large effect on the structure of short linear polypeptide chains. The crystallographic analysis of these biomolecules is hampered by this conformational dynamics and, even within the same crystallising solution, crystals with different unit cell dimensions have been observed [15]. In order to study the functional mechanisms of peptides in a sensible manner, therefore, the choice of experimental parameters is essential. The 26-amino-acid amphipathic peptide melittin, for example, adopts different degrees of helicity and varies in its tertiary fold when investigated by X-ray crystallography [16], NMR spectroscopy in organic solution [17,18], in the presence of micelles [19,20], or in association with lipid bilayers [21,22]. Polypeptides strongly associated with phospholipid bilayers have been investigated by solid-state NMR spectroscopy. This technique provides information on the secondary structure, the orientation and penetration with respect to the membrane surface (topology), as well as the peptide dynamics (e.g., [23]). In addition, the effects of membrane-associated peptides on the macroscopic phase properties of the membranes, the lipid head-group conformations or the fatty acyl chain packing have also been studied by solid-state NMR spectroscopy (e.g., [24–26]). The characterisation of peptide–lipid interactions by structural methods including solid-state NMR spectroscopy, therefore, forms the basis from which mechanistic models for antibiotic and pore-forming activities can be developed.

2. Solution and solid-state NMR spectroscopy to investigate membrane peptides

The solubility of amphipathic or hydrophobic polypeptides is often insufficient in aqueous buffers for investigating these biomolecules by solution NMR spectroscopy, and organic solvents have therefore been used. Mixtures with trifluoroethanol (TFE) are thought to mimic the membrane environment more closely than water alone, since TFE is moderately hydrophobic and known to enhance the inherent helical propensities of polypeptides [27]. However, the use of detergent micelles in aqueous buffers seems a much better choice when the membrane interface is to be simulated during solution NMR experiments [19]. Since the correlation times of DPC or SDS micelles are similar to those observed for large soluble proteins of 20–30 kDa, ^{1}H NMR spectra of small peptides in micellar solutions are characterised by resonance line widths of typically 15–30 Hz [23,28,29]. Thus spectral overlap and the lack of direct information on J-couplings makes the conformational analysis of peptides in micellar environments more difficult and the resulting structures are usually less well defined. Nevertheless, several peptide antibiotics have been investigated in the presence of detergent micelles using solution NMR spectroscopy [7,30,31].

Whereas molecules in solution quickly reorient retaining only their 'isotropic' values, the nuclear interactions with the magnetic field are inherently anisotropic [32]. The correlation times of small peptides associated with large macromolecular assemblies, such as phospholipid membranes, are to a large extent determined by the size of the complex. Tumbling is, therefore, considerably slower when compared to this same peptide in solution. In order to obtain information about the structure and dynamics of peptides associated with extended lipid bilayers, solid-state NMR spectroscopic methods have been developed.

The anisotropic contributions of the chemical shift, the dipolar and the quadrupolar interactions often constitute the most pronounced features of solid-state NMR spectra. The ^{15}N chemical shift anisotropy of a single static site, for example, covers approximately 175 ppm [33,34] (Fig. 1C). This is an order of magnitude greater than the dispersion

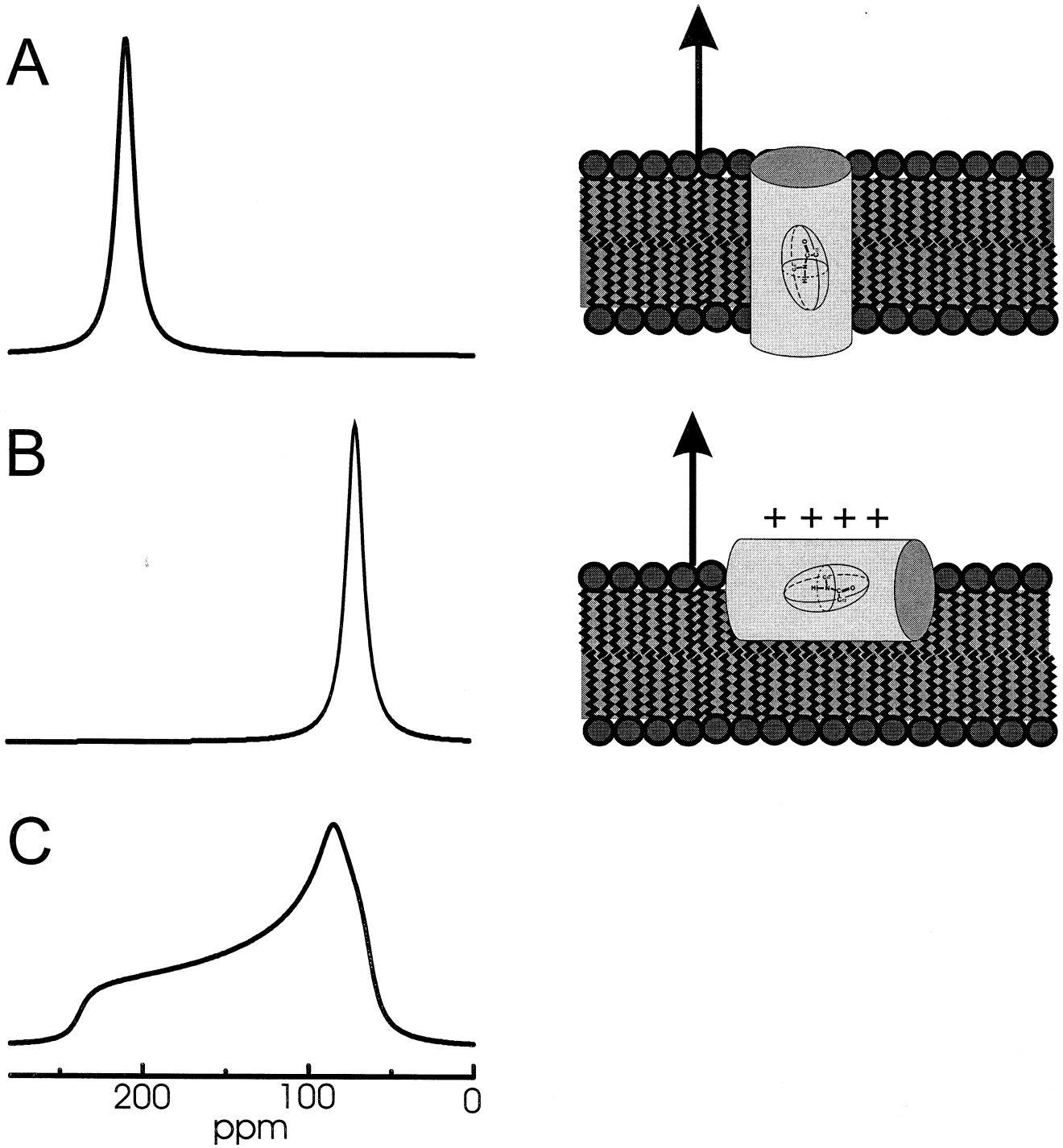

Fig. 1. Calculated proton-decoupled ^{15}N solid-state NMR spectra of helical peptides ^{15}N-labelled at a single site and reconstituted into oriented membranes (illustrated to the right of the spectra). The membrane normal is aligned parallel to the magnetic field direction (arrows). (A) Transmembrane orientation of the helix axis. (B) Orientation of the peptide approximately perpendicular to the magnetic field direction. (C) Powder pattern line shape where a random distribution of molecular orientations has been assumed. The ^{15}N chemical shift is scaled to liquid NH_3.

in the isotropic ^{15}N chemical shift dimension observed for the amide bonds of a protein in solution (15 ppm). The resulting broad lines of immobilised samples tend to show a high degree of signal overlap when they are merely transferred into test tubes and solid-state NMR spectra recorded. On the other hand, the magnitude and the orientational dependence of nuclear interactions provide valuable information about the dynamics, the molecular structure, and the orientation of peptides associated with lipid bilayers.

In order to illustrate the orientational dependence of the solid-state NMR spectra measured from static, oriented samples, Fig. 1 shows simulations of ^{15}N NMR spectra recorded from membrane-associated peptides labelled with ^{15}N at a single amide bond. The anisotropic chemical shift interactions are mathematically described by second rank tensors. The amide ^{15}N chemical shift tensor embedded within the chemical structure of an α-helix are represented graphically by an ellipsoid in Fig. 1A,B. The three main axes of the ellipsoid represent the main tensor elements σ_{11}, σ_{22} and σ_{33}. The chemical shift that is measured at a certain orientation of the molecule corresponds to the length of a vector parallel to the magnetic field direction, starting at the centre of the ellipsoid and ending at the intersect of the magnetic field vector with the coat of the ellipsoid. Fig. 1A exhibits a situation where the long axis of the ellipsoid (σ_{33} component of the ^{15}N chemical shift tensor) is aligned close to parallel to the NH bond vector/helix axis. The molecules, therefore, exhibit ^{15}N resonances at values >200 ppm (Fig. 1A). The short axes of the ellipsoid (σ_{22} and σ_{11} main tensor elements) correspond to chemical shifts of 85 ppm and 65 ppm, respectively [33–35]. Chemical shifts in this order of magnitude, therefore, indicate that the magnetic field direction is oriented within the plane defined by the σ_{11} and σ_{22} vectors, i.e., perpendicular to the main axis of α-helical conformations. Fig. 1A,B illustrates the functional dependence of ^{15}N chemical shifts for helical peptides. It should be noted, however, that the conformational analysis of membrane-associated polypeptides by oriented solid-state NMR spectroscopy is not limited to the presence of helical secondary structures, as the nuclear interactions exhibit a functional dependence on the alignment of chemical groups, such as the amide bond, with respect to the magnetic field direction. If the secondary structure of the peptide is known from CD, FTIR, Raman, solution, or solid-state NMR spectroscopies (reviewed in, e.g., [6,7]), the ^{15}N chemical shifts suffice to approximately orient the polypeptide domains with respect to the surface of uniaxially aligned lipid bilayers (Fig. 1A,B) [36–39]. Samples in which all orientations in space are present exhibit 'powder pattern' line shapes (Fig. 1C). These are composites of the resonances of all individual molecules and their line shapes are, therefore, determined by the molecular distribution as well as by the functional dependence between the chemical shift and the molecular orientation.

A detailed analysis of protein structures from solid-state NMR measurements requires that the size of the main tensor elements, as well as their direction within the molecular co-ordinate system, are known. The proton-decoupled ^{15}N chemical shift tensors for alanine or glycine amides have been studied in considerable detail for a large series of polypeptides [34,35,40–42]. These tensors show some modest dependence on the secondary structure of the polypeptide chain and the nature of the amino acid side chain. Small variations in the tensor elements have been included into the error margin during quantitative analyses of tilt angles from static solid-state NMR spectra [36,39].

The dipolar coupling between two nuclei is another important interaction that exerts a strong influence on the appearance of solid-state NMR spectra and which has been used to derive structural information. The dipolar interaction D is a function of the distance r between these nuclei, and the angle Θ of this vector r with respect to the magnetic field direction:

$$D \propto \frac{3\cos^2\Theta - 1}{r^3}$$

When samples are mechanically rotated at high speeds around the 'magic angle', the anisotropic contributions of dipolar and chemical shift terms cancel ($3\cos^2\Theta - 1 = 0$ at $\Theta = 54.7°$), causing magic angle spinning (MAS) NMR spectra to resemble 'isotropic' spectra [32]. The ^{15}N and ^{13}C chemical shifts have been used to determine the structure of the polypeptide main chain [41,43]. Important structural information, including the size of the dipolar coupling or

the molecular orientation in space are, however, lost. Therefore, magic angle spinning NMR techniques have been developed that selectively reintroduce the dipolar interaction term (reviewed in [44–46]).

Whereas peptide dynamics have been studied in non-oriented samples [23,31,35,47], investigations of the conformation and topology of polypeptides by static NMR techniques requires the uniaxial orientation of membranes with respect to the magnetic field direction. Phospholipid membranes orient mechanically when applied onto glass plates [48], or magnetically when phospholipids are mixed with bicelle-inducing detergents [49]. This latter approach requires a careful adjustment of the sample temperature and composition. Interesting new developments suggest that the magnetic alignment of lipid bilayers will become a versatile approach for the uniaxial orientation of hydrophobic polypeptides in membranes [50,51]. Till now, however, solid-state NMR spectroscopy has relied heavily on the preparation of mechanically aligned samples. After the polypeptide–lipid mixtures have been applied onto several thin cover glasses of, for example, 11×22 mm, the samples are equilibrated for several days in an atmosphere of defined humidity (typically $>90\%$ r.h.) and stacked on top of each other. The resulting oriented lipid bilayers are well hydrated, although bulk water in between the hydration shell of the lipids is absent. The lipid binding equilibria, therefore, tend towards the membrane-associated state and the peptides exhibit anisotropic mobility. When well-aligned membranes are introduced into the NMR spectrometer with the bilayer normal parallel to the magnetic field direction (B_0), the main axis of rotational diffusion coincides with the B_0 vector. This set-up avoids the introduction of additional peptide orientations concomitant with broadened resonances from rotational diffusion. The line shapes of these NMR spectra are a function of the orientational distribution of molecules with respect to the magnetic field direction (mosaic spread), contributions from conformational heterogeneity and the dynamic interchange between different membrane topologies [23,28,39].

2.1. The gramicidin A structure by solid-state NMR spectroscopy

Although hopes were initially raised that gramicidin A, a 15 residue peptide of the soil bacterium *Bacillus brevis*, would be useful as a cure against mortal infections such as tuberculosis, it has proven to be too toxic for application as a therapeutic agent [52,53]. Nevertheless, a short discussion of this peptide is included in this review. It was the pioneering work of Tim Cross and co-workers who, using this molecule in oriented phospholipid bilayers, demonstrated that solid-state NMR spectroscopy is capable of determining complete structures of membrane polypeptides at atomic resolution. To our knowledge the structure of gramicidin A is so far the first and only conformation submitted to a protein database that has been determined solely from solid-state NMR spectroscopic data. The detailed understanding of the structure and dynamics of the gramicidin channel in lipid bilayers provides a sound basis to understand how ions are selected and transported across membranes in a controlled manner. Whereas the ^{15}N chemical shift information from oriented membrane samples alone is sufficient to determine the approximate alignment of secondary structure elements with respect to the membrane surface [36,37], measurement of more than one interaction per peptide bond allows for a detailed analysis of the peptide secondary structure. Using oriented solid-state NMR spectroscopy, the ^{15}N–^{1}H (or ^{15}N–^{2}H) and ^{15}N–$^{13}C_1$ dipolar couplings have been determined from singly or doubly labelled gramicidin A samples, respectively. From this information possible orientations of the peptide plane with respect to the magnetic field direction (bilayer normal) were calculated [54,55]. The ^{15}N and ^{13}C chemical shifts [54,56], ^{2}H quadrupolar splittings [57,58] as well as the known geometries of peptide bonds were used as additional structural filters to reduce the number of possible solutions [55]. When consecutive peptide bonds are linked together, the tetrahedral geometry about the Cα position and information about the Cα–^{2}H orientation further reduce the number of possible solutions to a small set of four torsion angular pairs ϕ/Ψ. For gramicidin all ϕ/Ψ solutions are located in the β-region of the Ramachandran plot [54,55,57,59]. Ambiguities remain as the measured solid-state NMR parameters are indifferent to the magnetic field pointing up or down in laboratory frame (chirality) as well as to rotation of the dipolar vectors around the magnetic field direction. Although several discrete solu-

tions for the orientation of each amino acid residue are selected by this initial analysis, only four closely related structures of the gramicidin molecule remain after assembling together the peptide planes [54,55]. Structural refinement was performed using 120 orientational backbone constraints and hydrogen bonding distances. In order to carry out these calculations, some of the initial assumptions such as fixed geometry and perfectly planar structure of the peptide bond were relaxed, and this resulted in a single averaged structure [55]. Gramicidin A assumes a transmembrane right-handed β-helix with 6.5 residues per turn when reconstituted into membranes [55]. This unusual polypeptide conformation is the result of alternating L- and D-amino acids in the gramicidin A sequence. As one of these helices is capable of spanning a lipid monolayer only, head-to-head dimerisation results in a stable transbilayer pore (26 Å).

In order to accurately calculate structural parameters from the chemical shift information of oriented spectra, knowledge of the effective tensor in the peptide environment is required. The detailed investigation of the ^{15}N chemical shift interaction tensors has been achieved using non-oriented samples of synthetic peptides labelled at single sites and reconstituted into hydrated membranes. Whereas the backbone tensors of gramicidin A show little orientational variation within the molecular frame ($< \pm 2°$) [60], the chemical environment as well as global and local motional averaging affect the size of the tensor interactions [35,60]. These tensor characterisations not only made the accurate interpretation of orientational constraints possible, at the same time, the detailed dynamics of the labelled sites were also determined. The availability of single-site labelled samples from chemical peptide synthesis has been of key importance in these studies, as at present it is not possible to obtain this important set of data from samples with multiple labels.

Furthermore, the conformation, dynamics and orientation of all side chains of gramicidin A were determined. This was achieved by oriented ^{2}H solid-state NMR of deuterated valine [61,62] and leucine residues [54]. In addition, the structure of the tryptophan side chains has been studied by ^{13}C, and a combination of ^{15}N and ^{2}H solid-state NMR spectroscopies [63,64]. Solid-state NMR spectroscopy alone, however, did not always provide sufficient information to unambiguously resolve the structure of these side chains. In these cases the restraints, together with torsion angle energies, allowed the selection of the 'most probable' conformations.

The gramicidin A channel supports a single-file column of water inside its 4 Å wide pore. Passage of an ion, therefore, requires replacement of one of these water molecules and correlated movement of ions and water through the channel. Whereas the presence of anions does not show any effect on the solid-state NMR spectra of gramicidin, monovalent cations exhibit a pronounced influence on the chemical shifts of the most water-exposed carbonyls of Leu10, Leu12 and Leu14 [65,66]. However, other amino acids, as well as the tryptophan side chains, remain largely unaffected by the addition of cations [63,66]. Due to the large channel diameter and the polarisation effects observed in the presence of monovalent cations, it has been concluded that the monovalent cation binding site is delocalised over the interaction volume of the Leu10, Leu12 and Leu14 carbonyls. The lack of large structural alterations at the primary binding site of the ion prevent a deep potential energy well which would result in a reduced dissociation rate [66]. The carbonyls merely replace water molecules and, upon penetration of the ion into the channel, dehydration has been suggested to occur in an incremental manner until only two of six water molecules of the primary hydration sphere remain associated with the ion [66]. The helical arrangement of backbone carbonyls around the inner channel wall is suggestive for an off-axis helical transport pathway through the pore [67]. The tight association of water molecules with divalent cations provides a mechanism to prevent passage of these ions. A related ion selectivity filter has been detected in the X-ray structure of the 17.6 kDa KscA potassium channel from the soil bacterium *Streptomyces lividans* [68]. This protein forms a tetrameric arrangement in which selectivity for K^+ is achieved by specific interactions of this ion with the main chain carbonyls of a 12 Å long region (instead of, e.g., charged side chains).

The global rotational reorientation of gramicidin A is temperature dependent and occurs at correlation times of approximately 10^{-9}–10^{-4} s [69–73]. The local dynamics of gramicidin A have been investigated

with the help of field-dependent T_1 relaxation measurements on oriented peptide samples in liquid crystalline lipid bilayers [74]. Librational motions of approximately ±6° around the Cα–Cα axis of adjacent amino acids occur on a 10-nanosecond time scale, thereby correlating with the time scale of translocating ions from one carbonyl to the next [74]. Furthermore, picosecond and subpicosecond dynamics around the same axis reduce the σ_{22} and σ_{33} components of the powder patterns [35]. These backbone librations occur with amplitudes of ±14° to ±22° at low temperatures (< 263 K) and strongly increase at the final turn of the helix above the ice melting temperatures (283 K). Librations of carbonyls into the channel lumen seem important as they allow the passing sodium ions to maintain a solvating environment.

Studying the tryptophan indole ^{15}Nε powder patterns as a function of temperature indicates that these side chains, although fixed in a rotameric state, exhibit librations of the tryptophan side chains by 19–29° around the χ_2 axes. These side chain dynamics modulate the dipolar interaction strength which is effective at the channel mouth by about 4 kJ/mol [75,76]. Such fluctuations could form a rapid gate for conductance by helping to release the ion into the pore. At the same time significant components of the tryptophan indole dipole moments reduce the rate-limiting energy barrier for ion passage at the monomer–monomer junction in the centre of the pore [76,77]. By reviewing the solid-state NMR data, it becomes clear that the detailed analysis of the structure and dynamics of the gramicidin A channel, although of simple and unique composition, has provided many valuable insights into the mechanisms of transmembrane channel formation.

In contrast to the transmembrane alignment of gramicidin A dimers, the solid-state NMR structural data measured from the antibiotic peptide magainin 2 are only in agreement with a right-handed α-helix when compared to other low-energy secondary structures [78]. The helix axis of this polypeptide is oriented parallel to the membrane surface and, therefore, does not reach through the bilayer. The puzzling question of how this peptide forms pore-like structures will be addressed in the next section.

2.2. *Linear peptide antibiotics from insects and amphibians*

As pathogenic organisms become increasingly resistant to the commonly applied antibiotics, there has been considerable interest in discovering and exploring the utility of natural antibiotic peptides by themselves, or as templates to design derivatives for pharmaceutical and agricultural purposes [14,79,80]. Amphipathic peptides are found in many species including insects, amphibians, humans or plants (recently reviewed in [3–6,9,10,80,81]). These peptides show bactericidal, fungicidal, virucidal and tumoricidal activities without lysing cells of healthy eucaryotes (e.g., [82–84]). The best studied of these peptides are probably the members of the bombinin-magainin (or 'PGS') family first found in toads and frogs [85–87], and the cecropins isolated from the pupae of the cecropia moths [88,89]. Polypeptide sequences are shown in Table 1. A 31-amino-acid mammalian analogue, cecropin P, has also been isolated [90,91]. Whereas magainins are stored in granula in the skin of frogs, cecropins are induced upon infection. Both these peptide families, therefore, provide a fast innate host defence system [1,2]. The ac-

Table 1
Amino acid sequences of channel-forming peptides

KWKLF KKIEK VGQNI RDGII KAGPA VAVVG QATQI AK–$CONH_2$	Cecropin A
GMASK AGAIA GKIAK VALKA L–$CONH_2$	PGLa
GIGKF LHSAK KFGKA FVGEI MNS–$CONH_2$	PGS (Magainin 2)
KWKLF KKIGI GKFLH SAKKF–$CONH_2$	CA(1–8)–MA(1–12)
KWKLF KKIGI GAVLK VLTTG–$CONH_2$	CA(1–8)–ME(1–12)
GIGAV LKVLT TGLPA LISWI KRKRQ Q–$CONH_2$	Melittin
KKALL ALALH HLAHL ALHLA LALKK A–$CONH_2$	LAH_4
Ac–UPUAU AQUVU GLUPV UUEQF–OH	Alamethicin

U, α-methylalanine; $CONH_2$, C-terminal carboxyamine; OH, C-terminal amino alcohol; Ac, N-terminal acetyl.

tivity of naturally occurring combinations of some members of this peptide family, such as PGLa and magainin 2, are more potent than the equivalent amounts of either of these peptides alone, indicating a synergistic enhancement of activity [92–94]. Similarly, cecropin–melittin or cecropin–magainin hybrid peptides are more active by up to two orders of magnitude in antibiotic assays when compared to native cecropins [95,96]. The peptide hybrids nevertheless retain the lack in haemolytic activity.

Both magainins and cecropins have been shown to exhibit pronounced effects on cellular energy metabolism, suggesting that they exhibit their cytotoxic activity by disrupting the electrochemical gradient across energy-transducing membranes [97–99]. The presence of 0.6–3 mol% magainin 2 results in the half-maximal decoupling of the respiratory free-energy transduction of bacterial or spermatozoal cells, isolated mitochondria, or reconstituted cytochrome oxidase liposomes ([100] and refs. cited therein). However, no simple correlation has become evident between antibacterial activity and the uncoupling of the respiratory phosphorylation in mitochondria when the concentration dependent effects of cecropins have been tested [98]. A high coverage of bacterial membranes has been detected when radioactively labelled cecropins develop their bacteriotoxic activity [101]. Resistant bacteria, however, are loaded with cecropins to a similar extent whereas non-permissive erythrocytes are not. Therefore, factors other than merely the binding affinity must also play an important role in determining the susceptibility of cells to these bacteriotoxins [98,101].

All-D-magainins, *all*-D-cecropins, cecropins with inverted sequences (retro) or inverse D-cecropins (retro-enantio), all possess the high antibiotic and the pore-forming activities of the parent L-enantiomer [13,102,103]. These findings indicate that the cell-killing activities of these amphipathic peptides are not mediated through specific, chiral receptor interactions. Direct peptide–lipid interactions have, therefore, been suggested as being the underlying mechanism for the peptides' biological activities.

Electrophysiological investigations of planar model membranes indicate that the conductivity for ions augments in the presence of cecropins or magainins [104–107]. The increases in step-wise conductivity during electrophysiological experiments described by some authors [104,105,108] was taken as an indication for pore formation by transmembrane helical bundles [109–112], in analogy to the mechanism proposed for the hydrophobic peptide alamethicin [6,113] (Fig. 3A). A large range of conductivities of the pores, starting at 1.8 pS and ranging over three orders of magnitude, has been detected for magainin 2 [105,108]. The size of these channels varies within each electrophysiological recording as well as from experiment to experiment. Whereas magainin 'channels' in PC/PE 7:3 membranes are anion-selective (ratio $P_K/P_{Cl} = 1:3$) [108], a selectivity of cations over anions (5:1) exists in mixed PE/PS 1:1 membranes [105]. Small anion selectivity (Cl^-/Na^+ 2:1) was also observed for the large channels (2.5 pS) formed by cecropin AD [104]. Selectivity within the respective class of monovalent ions was not detected in any of the published electrophysiological experiments. In addition, these channel events are rare and short lived [105,107,108]. Magainin-induced electrophysiological events have, therefore, been described as 'occasional brief multilevel fluctuations' (at 0.1 mg/ml), or, at higher peptide concentrations, as 'melittin-like bilayer disruptions' [107].

In the absence of transmembrane potentials, magainin or cecropin-magainin peptides have been shown to cause the release of the fluorescence dyes calcein (M_r 623) or 6-carboxyfluorescein/Co^{2+} from large or small unilamellar vesicles [114–116]. Similarly, a cecropin A–melittin hybrid permeabilises mitochondrial inner membranes both in the presence or absence of transmembrane potentials [117]. Interestingly, the permeability of ions increases already at lipid-to-cecropin ratios >200; the release of fluorophores from vesicles or of cellular constituents, on the other hand, requires much higher amphiphile concentrations [10,99,118].

Magainin (PGS) polypeptides consist of 21- to 26-amino-acid residues some with strongly basic character. These peptides dissolve well in aqueous solution where they assume random coil conformations. They also show a strong affinity for phospholipid membranes where they assume right-handed α-helical conformations (Fig. 2, reviewed in [6]). Interestingly, this lack of secondary structure before membrane insertion seems an important factor for efficient antibiotic activity of cationic peptides [119]. On the other

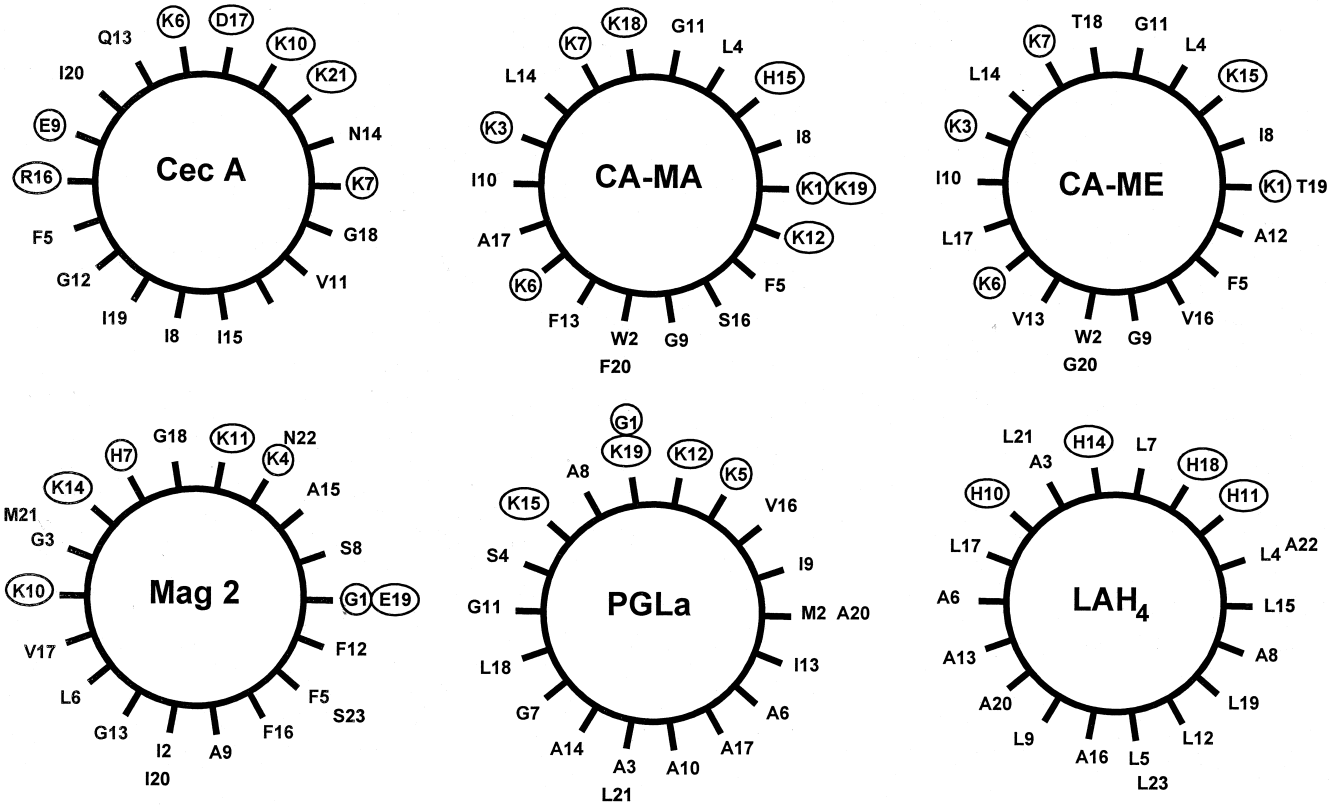

Fig. 2. Edmundson helical wheel diagrams of cecropin A (residues 5–21); CE-MA: cecropin A(1–8)–magainin(1–12); CE-ME: cecropin A(1–8)–melittin(1–12); PGS (magainin 2); PGLa; and LAH_4 (residues 3–23). Charged amino acids are circled.

hand, the cell-lytic activities of cecropins correlate with the formation of α-helical secondary structures in membrane environments as well as with their binding affinity to liposomes [120].

MAS solid-state NMR distance measurements using the ^{15}N decouple, ^{13}C detect REDOR technique were used to measure intramolecular distances between labelled sites of magainin 2 and agree with α-helical conformations of magainin 2 in the presence of DPPG/DPPC 1:1 bilayers [121]. At high peptide-to-lipid ratios, however, α-helix and β-sheet contributions have been shown to co-exist using ATR–FTIR and ^{13}C MAS–NMR spectroscopies [121]. For these experiments the lipid-to-peptide ratio was as high as 11.4 (mol/mol) and the samples had been lyophilised, frozen or the lipids were in their gel phase, respectively.

Similarly, cecropin A assumes a predominantly random coil conformation in water [88,122]. In 15% hexafluoroisopropanol (v/v) cecropin A exhibits two α-helical regions (residues 5–21 and 24–37) that are interconnected by a flexible hinge region near proline 24 [123]. Whereas the central part of the C-terminal helix (residues 25–33) is hydrophobic, the length and the continuous distribution of basic residues along one face of the amphipathic N-terminal helix closely resembles the amino acid distribution of magainins (Fig. 2). Similar structures in organic solvents are also found for a mixed peptide consisting of the first 13 N-terminal amino acids of cecropin followed by the 13 N-terminal residues of melittin [79,124], or cecropin-like peptides [125–127]. The mammalian analogue cecropin P, on the other hand, lacks the flexible hinge region [128]

In order to analyse the structure and alignment of magainin antibiotic peptides in planar lipid bilayers, proton-decoupled ^{15}N solid-state NMR spectroscopy has been performed on oriented samples of magainin 2 [78] and PGLa [31]. Several peptides have been synthesised by chemical methods, each labelled at a single residue throughout their sequence. The pep-

tides have been reconstituted into mechanically aligned bilayers, equilibrated at 93% relative humidity and introduced into the solid-state NMR spectrometer with the membrane normal parallel to the magnetic field direction. The ^{15}N chemical shifts of eight labelled residues of magainin 2 occurred around 80 ppm (relative to liquid NH_3), indicating an orientation of the NH vector approximately perpendicular to the magnetic field direction (membrane normal). Additional multidimensional solid-state NMR experiments allowed for the measurements of both the proton-decoupled ^{15}N chemical shift, the ^{1}H chemical shift, as well as the ^{1}H–^{15}N dipolar coupling of four consecutive residues (14–18) [78,129]. All measured parameters are dependent on the orientation of the labelled peptide bond with respect to the magnetic field direction and can, therefore, be used to calculate the secondary structure of this region when associated with lipid bilayers. Only right-handed α-helical conformations agree with the measurements among all low-energy secondary structures tested [78]. Proton-decoupled ^{15}N solid-state NMR spectra obtained at magainin 2 concentrations of 0.8–3 mol% from eight residues between positions 2 and 20 suggest that in lipid bilayers the α-helix extends to the terminal regions of the peptide [78]. Edmundson helical wheel analysis shows that such a helix is amphipathic with the polar and hydrophobic amino acid side chains separated on opposite faces of the helix (Fig. 2). Intercalation of this helix into the bilayer interface in an in-plane fashion, therefore, allows for both hydrophobic and electrostatic interactions to be satisfied.

The extension of helical structures into the peptide terminal regions, as observed by oriented solid-state NMR spectroscopy, seems to contrast the much lower degree of helicity derived from optical spectroscopies. These latter techniques, however, test for the conformational average of peptide dissolved in the water phase (random coil) and peptide associated with the membrane (highly α-helical). As these measurements are performed with dilute samples, the presence of negatively charged lipids is required to enhance the membrane affinity of the basic peptides by electrostatic attraction [130]. In contrast, the oriented samples used in solid-state experiments are characterised by a reduced bulk water content and the experimental set-up allows one to focus on the immobilised polypeptide sample by using cross-polarisation pulse sequences [131].

The ^{15}N chemical shifts obtained from oriented magainin 2 samples furthermore indicate that the α-helix is oriented with its long axis parallel to the membrane surface [36,37]. This in-plane alignment has been observed for a wide variety of lipid compositions, including bilayers of POPE/POPG 3:1 or POPC/POPG/cholesterol 3:1:4, i.e., with lipid compositions that mimic procaryotic and eucaryotic membranes, respectively [26]. In-plane orientations of magainin 2 at 3 mol% concentrations have also been observed by ATR-FTIR spectroscopy in dry oriented samples [132] and by oriented CD spectroscopy [133]. In addition, fluorescence quenching experiments of magainin derivatives, where the three phenylalanines of magainin 2 are independently replaced by tryptophans, confirm the in-plane orientation observed with ^{15}N solid-state NMR spectroscopy [134]. These experiments indicate that all three fluorescent probes are localised approximately 10 Å equidistant from the bilayer centre. Peptide insertion into the membrane was also monitored by photolabelling techniques [135]. The solid-state NMR results were taken as an input to optimise computer programmes which use molecular simulations to determine the conformation, penetration and orientation of bilayer-associated peptides [136,137]. The localisation of these peptides at the membrane surface have furthermore been confirmed by fast deuterium exchange monitored by FTIR spectroscopy as well as REDOR magic-angle spinning solid-state NMR spectroscopy [121]. The latter experiments indicate a close distance between labelled ^{13}C residues in the centre of the peptide and the immobilised head groups of DPPC/DPPG 1:1 membranes. This data contrasts the results obtained by oriented CD spectroscopy, which indicate transmembrane helix alignments in the presence of DMPC/DMPG 3:1 at full hydration and peptide concentrations >3 mol% [133]. Topological differences may be due to experimental parameters such as hydration and lipid composition. Alternatively, the possibility remains that at high peptide-to-phospholipid ratios macroscopic phases different from extended lipid bilayers exist which explain both experimental findings.

Multidimensional solution NMR spectroscopy in micelles, in combination with solid-state NMR spec-

troscopy on phospholipid bilayers, indicates that the peptide antibiotic PGLa also assumes α-helical conformations that are oriented parallel to the membrane surface [31]. X-ray diffraction experiments provide supporting results [138]. Whereas the C-terminus of this peptide strongly associates with lipid bilayers, the local dynamics in the presence of POPC increases toward the N-terminus in agreement with helix propensity calculations [138]. The narrow anisotropies of the proton-decoupled ^{15}N spectra of unoriented samples which is observed for ^{15}N-Ala3 and ^{15}N-Ala6, indicate that these residues of PGLa exhibit a high degree of mobility on the time scale of the solid-state NMR experiments (10^{-3}–10^{-4} s). This result also indicates that at 93% r.h., the hydration of oriented bilayer stacks is sufficient to allow the reorientational freedom of the peptide terminus. Using double D-amino acid replacements, the α-helical conformations of the magainin 2 N-terminus were also shown to be less stable in the presence of liposomes when compared to the C-terminus [139]. Similarly, the C-terminus of cecropin(1–8)–magainin(1–12) hybrids exhibit a higher propensity to form helical structures when compared to the N-terminus [140]. Taken together, these results suggest repulsive interactions between the positive pole of the helix dipole (N-terminus) and charged lysine side chains that destabilise the helix conformation.

ATR–FTIR spectroscopy and molecular dynamics calculations show that the continuous helix of cecropin P [128] exhibits orientations parallel to the membrane surface as well [141,142]. Similarly, cecropin A is predominantly oriented in the plane of lipid bilayer stacks [143]. The structural and functional similarities between several cecropins, PGLa and the magainins suggest that these develop their antibiotic and pore-forming activities by similar mechanisms. The importance for biological activities of residues within the amphipathic N-terminal helix, as well as within the flexible linker region of cecropin, seems to support such a suggestion [101,104,122,144]. The long list of related sequences might further include other amphipathic peptide antibiotics such as Abp3 [126], bombinin [85,145], bombolitin [146], buforins [147], caerin [148], ceratoxins [127], dermaseptins [10,149], gaegurins [150], maculatin [151], pexiganan [152], PMAP-37 [153], Shiva-3 [154], and designed sequences [139,155,156].

Although the secondary structure and the functional properties of cecropins and magainins have been characterised by a multitude of techniques, the mechanism of antibiotic action and increases in electrical conductivity across lipid bilayers is still a matter of speculation. In fact, there seems to be a discrepancy between the experimental data indicating in-plane alignments of amphipathic peptides and the suggested formation of channels by transmembrane helical bundles. This discrepancy would be reconciled if the majority of the peptides resided on the membrane surface with only a minor fraction interacting in a transmembrane fashion, or if other models were to be applied [6]. In order to evaluate these possibilities, a quantitative understanding of the peptide-peptide and peptide–lipid interactions in membranes is necessary. With the estimated Gibbs free energy of transition between in-plane monomers and channel-forming transmembrane aggregates, the equilibrium constant and the ratio of peptide populations in transmembrane versus in-plane alignments can be calculated [23]. This result allows the comparison of the estimated probabilities of channel formation with experimental results.

2.3. *Amphipathic model peptides with pH-dependent orientations*

Amphipathic model peptides not only exhibit pronounced antibiotic activities [156–158], but they also allow one to study in considerable detail the various interaction contributions relevant for peptide topological order [6,23]. In order to better understand the mechanisms of pore formation and antibiotic activities of amphipathic peptides, α-helical sequences have been designed in our laboratory. These helices are characterised by a hydrophobic face separated from a more polar region of variable composition 'X' by four histidines (Fig. 2). The polarity of these histidine side chains is strongly dependent on the pH of the surrounding medium, therefore many of these peptides exhibit pH-dependent transitions between transmembrane and in-plane alignments [23,132,159].

Assuming a simple two-state equilibrium for the reorientational process, the equilibrium constant is calculated according to $K = [TM]/[IP]$, where [TM] is the concentration of transmembrane peptide and [IP] the concentration of peptide in in-plane align-

ments [23]. The Gibbs free energy that governs such a process is calculated according to the equation:

$$\Delta G = \Delta G^{h} + \Delta G^{d} + \Delta G^{p} + \Delta G^{\#},$$

with ΔG^{h} being changes in hydrophobic interactions during the transfer process, ΔG^{d} the energy required to discharge an amino acid side chain at a given pH, ΔG^{p} the contribution of placing a polar but uncharged side chain in the hydrophobic membrane interior, and $\Delta G^{\#}$ the sum of changes in all other interactions such as hydrophobic mismatch energies, the energies of fatty acyl chain conformational changes during the adaptation to the polypeptide surface, the lipophobic effect [160], or van der Waals interactions that occur during the process in-plane → transmembrane. Inherent in the above equation is the assumption that it is more favourable to remove the charge from an amino acid side chain before placing it in the bilayer interior. This notion is supported by comparing the Born energy of placing a charge in a low dielectric environment [161] with the sum of the energies of discharging an amino acid at neutral pH and consecutively placing a polar but uncharged residue in the membrane interior [6,23]. From the chemical potentials of the Lewis acid or base of amino acid side chains, it is possible to calculate the energy to discharge a base at any given pH according to:

$$\Delta G^{d} = n_i\, RT \ln r + 2.3RT\sum_i (\mathrm{p}K_i - \mathrm{pH}),$$

where i represents the amino acids that are discharged, n_i their total number and $RT \ln r$ amounts to approximately 11.5 kJ/mol [6,23]. The energy required to discharge the histidines of our model peptide is, therefore, a linear function of the difference between the pK of the side chain and the pH of the environment.

LAH_4, the first peptide of this family, has been investigated by oriented ^{15}N solid-state NMR as well as ATR–FTIR spectroscopies [23,132]. For this peptide a transition midpoint of around $pH_{50} = 6.3$ has been determined by analysing either the chemical shift distribution or the dichroic ratio of the amide I and amide II bands. Two well-separated lines are visible in proton-decoupled ^{15}N solid-state NMR spectra, indicating that the transmembrane and the in-plane peptide populations exchange slowly on the NMR time scale (10^{-4} s). Interestingly, the antibiotic activity of this peptide is an order of magnitude more pronounced at pH 5.5 when compared to magainin 2 [156]. At low pH both peptides are predominantly oriented along the membrane surface [23,78]. When the pH is increased to neutral, LAH_4 changes into transmembrane orientations and at the same time looses much of its antibiotic activity [156]. Magainin 2 or the LAK_4 analogue of LAH_4 show pH-independent activity similar to that of LAH_4 at low pH. These results suggest that the antibiotic action of amphipathic peptides is independent of the formation of transmembrane helical bundles. This conclusion is further supported by the pronounced antibiotic properties observed for α-helices consisting solely of leucines and lysines (≥11 residues) or of small peptidomimetics which are too short to span the membrane [155,157,162]. These peptides exhibit a narrow orientational distribution parallel to the bilayer surface when investigated by proton-decoupled ^{15}N solid-state NMR spectroscopy [163].

The hydrophobicity of residues X located at the polar face of the peptide exhibit a strong influence on the transition pH of these peptides (at pH_{50}, $\Delta G = 0$). It has been shown, for example, that the transitions of leucine-containing peptides are shifted to lower pH when compared to alanine-containing peptides [159]. This effect has been used to calculate the relative hydrophobicities of single amino acids. In contrast to the commonly used hydrophobicity tables, this approach yields values for amino acids that are part of helical polypeptides in bilayer environments, instead of, for example, the transition energy of isolated amino acids between water and octanol [159].

Due to the importance of lysine residues in peptide antibiotics, the topological effects of this amino acid has been investigated in some detail using amphipathic model peptides. Peptides that consist of hydrophobic amino acids with more than three lysine residues in the central region of the α-helix orient along the membrane interface [164]. In the presence of only one lysine residue transmembrane alignments are observed. The latter result suggests that in a hypothetical in-plane orientation, the lysine side chain cannot snorkel to the surface without exposing a considerable fraction of hydrophobic residues. The resulting hydrophobic interactions are larger and op-

posite in sign than the transfer energy of lysine (water → membrane). Using the above formalism, the transfer energy of lysine is composed of a hydrophobic term which arises from four methylene groups, the energy to discharge a side chain at ($pK-pH$) = 3.5, and the polar energy needed to move an NH_2-group into the hydrophobic interior of the membrane [23,164].

2.4. Melittin

The peptide–lipid interactions of melittin (or mellitin), a peptide isolated from the European honey bee *Apis mellifera*, have been studied in considerable detail using a variety of techniques including solid-state NMR spectroscopy. Although this peptide is too haemolytic to be used as an antibiotic, the many experimental data which have been published for melittin exemplify important aspects of peptide–lipid interactions. In addition, the comparison of melittin with other antibiotic peptides provides a guideline that helps to understand how selectivity between haemolytic and antibiotic activities is achieved.

Melittin readily binds to red blood cells where the peptides cause an increase in permeability for sodium and potassium ions, as well as cell swelling and the release of haemoglobin [11,12]. Conductance changes and discrete multilevel conductances have also been observed in the presence of this peptide (reviewed in [8]). Melittin is characterised by 5–6 positive charges, four of which are at the C-terminus. Transferred NOE and deuterium exchange measurements indicate that in the presence of lipid bilayers, melittin adopts α-helical conformations between residues 6 and 10 as well as between 13 and 21 interconnected by a flexible bend due to proline 14 [21,22]. At low concentrations of peptide, the helix axis is predominantly oriented parallel to the membrane surface [21,165]. However, at peptide-to-lipid ratios of 1/12 to 1/14, oriented ^{13}C solid-state NMR spectroscopy of peptides (each labelled at a single site with ^{13}C in ten different locations between residues 2 and 20) agree with α-helical peptides that exhibit transmembrane orientations [166]. These investigations are in agreement with dynamical equilibria between the peptide orientations which are functions of the physical state of the membrane [167–169].

The bilayer structure of liquid crystalline phosphatidylcholine (PC) is retained unaltered in the presence of up to 5 mol% melittin. However, ^2H and ^{31}P solid-state NMR, as well as ATR–FTIR spectroscopy, indicate that the order parameters of the fatty acyl chains decrease due to the presence of peptide [8,24]. Furthermore, electrostatic interactions of ^2H-labelled phosphatidylcholine head groups with membrane-associated surface charges has been monitored in a quantitative manner using deuterium NMR spectroscopy [170,171]. In the presence of melittin the POPC interface senses an effective charge from the peptide of only about 2, although at neutral pH melittin retains 4–6 positive charges [25,172]. A superficial peptide insertion into PC membranes might allow for an efficient screening of charges in the aqueous phase.

In the presence of intermediate amounts of melittin (<5 mol%), reversible micellisation concurrent with magnetic orientation of the structures occurs at temperatures below the liquid crystalline-to-gel state phase transition of the pure lipid [24,173,174]. Freeze-fracture electron microscopy, light scattering and gel filtration indicate that disc-shaped micelles with an approximate diameter of 235 Å are formed. These were suggested as consisting of 1500 bilayer lipids which are surrounded by a melittin belt [173]. The observed bilayer deformations are probably a result of the increased volume in the head-group region when melittin intercalates into the membrane [16,175]. The disc-like PC micelles are metastable, however, and transform into lamellar structures. The fusion kinetics are dependent on the mismatch between the bilayer hydrophobic thickness and the length of the melittin helix and can last for several days [24,176].

At high peptide concentrations both gel and liquid crystalline bilayers are transformed into small objects. In the gel state, however, the bilayer disruptive properties are only observed after pre-incubation of large PC vesicles at temperatures above either the gel-to-liquid crystalline phase transition [173] or the pre-transition temperature [177]. With the help of stopped-flow fluorescence spectroscopy, the penetration of melittin into the hydrophobic region of the membrane has been identified as the rate-determining step during incorporation into liquid crystalline bilayers [178]. The melittin-induced macroscopic changes of sphingomyelin membranes are qualita-

tively similar to those observed for DPPC bilayers [179].

The melittin-induced interconversion of membrane structures during temperature alterations is less pronounced in the presence of cholesterol [177,180]. It has been suggested that a tightening of the membrane prevents the insertion of melittin into the bilayer and that the molecular shape of cholesterol counteracts the melittin-induced wedge effect. The presence of 30 mol% cholesterol, however, also stabilises previously formed disc-like micelles. It has been shown that cholesterol is redistributed between the lamellar and the micellar phase during temperature changes [180]. These molecules thereby provide a buffer for a lipid order parameter that corresponds to a constant disc hydrophobic thickness of 29 Å.

Whereas melittin disrupts PC bilayers into small structures, the peptide exhibits bilayer-stabilising effects when mixed with phosphatidylethanolamine membranes under conditions where the pure lipid arranges in a hexagonal phase (H_{II}) [181]. Using a variety of biophysical methods including NMR spectroscopy it has been estimated that the peptide is localised at the membrane interface with the tryptophan-19 residue close to the glycerol backbone in the presence of zwitterionic membranes [21,182–184]. The peptide, therefore, occupies a much larger space at the level of the zwitterionic phospholipid head groups. The combination of a membrane-inserted short hydrophobic N-terminal helix and a surface-anchored highly charged C-terminal segment was suggested as an explanation for the particularly pronounced wedge shape of melittin when compared to other amphipathic molecules [185].

In contrast to observations with zwitterionic membranes, for cardiolipin a transition of the bilayer into H_{II} (high temperature) or cubic phases ($< 40°C$) is observed due to the presence of melittin [186]. Membrane insertion of melittin results in a preference for inverted phases for this and other charged phospholipids, including DOPA (H_{II}) or egg-PG [187]. The melittin fluorescence emission spectra have been used to localise the W19 of melittin in the hydrophobic interior of cardiolipin membranes [188].

When the surface charge density in the vicinity of deuterium labelled phospholipids is monitored by ^2H solid-state NMR spectroscopy [170], it has been shown that the positive charges of melittin compensate for the negative surface charge density introduced by the anionic lipids in mixed DMPC/DMPS membranes (80:20 mol/mol). The ^2H NMR spectra indicate that the effects of the peptide and lipid charges cancel each other at a lipid-to-peptide-ratio of 5:1, a value that is close to that expected from a peptide carrying 5–6 positive charges [189]. Whereas this former ternary system remains homogeneously mixed, a partial phase separation in mixed DSPC/DPPG bilayers was detected by fluorescence and Raman spectroscopies [190]. Interestingly, acidic phospholipids or fatty acids provide stabilising effects on PC lipid bilayers when melittin is present [189,191,192]. Alterations in melittin membrane penetration depth and/or different phospholipid headgroup geometries provide possible explanations for these stabilising effects.

2.5. Alamethicin

Alamethicin is a 20 amino acid fungal peptide of *Trichoderma viride* (reviewed in [6,53,193,194]). The alamethicin sequence consists of mostly hydrophobic amino acids, including two prolines at positions 4 and 14. Structural analysis by X-ray crystallography [195], NMR spectroscopy in methanolic solution [196], or in the presence of SDS micelles [197] indicate that the peptide adopts helical conformations which are interrupted by the proline-14 residue. The helix-breaking motif G-X-X-P introduces a flexible hinge region [197–200] with a 3_{10} helical turn between V15 and L12 in the crystal [195]. NMR experiments indicate a less regular helix conformation or considerable conformational averaging of the C-terminal residues [196,197], in agreement with molecular modelling calculations [201,202]. FTIR, Raman and CD spectroscopies show that the degree of helicity is dependent on the physical state of the lipid [167], the lipid/peptide ratio [203] and the presence of transmembrane potentials [204].

CD and Raman spectroscopies indicate that the peptide alignment with respect to the surface of supported bilayers exhibits a complicated phase diagram which is dependent on peptide concentration, the detailed lipid composition, hydration, and the macroscopic phase of the membrane [167,205]. Proton-decoupled ^{15}N solid-state NMR spectroscopy was performed with alamethicin labelled with ^{15}N at the

alanine-6 position and incorporated into uniaxially DMPC bilayers at peptide-to-lipid ratios of 1:8 [206]. These experiments demonstrate that the peptide is aligned in a transmembrane fashion and exhibits rotational averaging around the membrane normal. The ^{15}N chemical shifts and ^{1}H–^{15}N dipolar interactions agree with an α-helical but not a 3_{10} helical conformation of the N-terminus. The effect of molecular oxygen and paramagnetic ions on ESR spin label studies indicates that the N-terminus of alamethicin, in an orientation parallel to the membrane normal, remains 16 Å distant from the headgroup phosphates of the opposing bilayer leaflet [207]. It appears that hydrogen bonding interactions of the less regular C-terminal helix anchor the peptide at the bilayer interface [196,197,199,208]

When added to lipid bilayers, the polypeptide exhibits voltage-dependent conductance changes similar to those seen in the presence of large voltage- or ligand-gated channel proteins (reviewed in [6,53,193]). Under well selected patch-clamp conditions more than 20 different channel states have been observed [209]. The open alamethicin pore has been suggested as consisting of 3–11 helical rods arranged around a water filled pore, that form 'transmembrane helical bundles' or 'barrel staves' [193]. The best support for these models is derived from the co-operativity observed in membrane partitioning isotherms of alamethicin [210] and channel formation [211], as well as the pattern of successive conductance levels, each a few milliseconds long [113,212]. Starting from the lowest observed values, the conductivity of the black lipid membranes increases fast and in well defined steps of a few hundred picosiemens. The step size becomes larger as the conductivity increases. Transitions of a specific size have not been observed in conjunction with other states [113,193,212]. The frequency of conductivity bursts increases with the applied voltage, indicating that the macroscopic voltage dependence of alamethicin arises from the initial formation of the lowest-level pore. These observations have been taken as an indication that the smallest conducting structures consist of trimers (19 pS at 1 M KCl [213]) or tetramers (88 pS at 0.5 M KCl [214]).

Analysis of the alamethicin multiple channel kinetics indicates that the conductance fluctuations occur on a millisecond time scale and within a burst of channel openings. In contrast, the initial formation and decay of the lowest conductance state is 10 to 100 times slower. The respective activation energies are 50 and 120 kJ/mol [215].

Geometrical considerations indicate that a channel which consist of, for example, 11 monomers results in a diameter of 25.5 Å and a conductivity of ≥4.4 nS. Such a big pore has lost most of the little cation selectivity that is observed for the smaller channels [193]. High ionic strength stabilises the lower conductance levels and increases the life times of all levels, probably by decreasing the electrostatic repulsion between monomers that arise from like charges and/or α-helical dipoles [216]. For example, a decrease in channel activity is observed when the C-terminus of alamethicin is chemically modified to carry three negative charges [217].

Various models for the molecular mechanism of alamethicin voltage gating are based on interactions of the alamethicin helix dipole with the electric field (reviewed in [6,53,194,218]). The dipole moment of alamethicin corresponds to a net +1/2 charge at the N- and a −1/2 charge at the C-terminus of the helix (75 Debye = 16 eÅ, [219]). Whereas in most of the suggested models voltage gating involves reorientation of part or all of the helix dipole, it has also been observed that partitioning of alamethicin from solution into the membrane increases with the applied transmembrane voltage [220].

3. Models for channel formation and antibiotic activity

3.1. The transmembrane helical bundle model

The 'classical' picture to explain formation of pores in planar lipid bilayers is the so-called 'barrel stave' or 'helical bundle model' (Fig. 3A). This model is often used to explain pore formation and step-wise conductivity increases in single-channel measurements. The best studied peptide for which the formation of transmembrane helical bundles has been suggested is alamethicin, a member of the family of peptaibols. In contrast to the openings observed with highly charged amphipathic peptides, the alamethicin channels are reproducible and well defined. The interested reader is asked to refer to the above discus-

sion on alamethicin to review important experimental details that form the basis of this model (cf. *supra*).

Channel formation has been shown to occur and oriented solid-state NMR spectroscopic measurements support formation of transmembrane helical bundles for the following peptides: HIV-1 protein U [39], the transmembrane region of the related M2 polypeptide of influenza A in the absence [38] and presence of the antiviral drug amantadine [163], or the putative channel lining fragment M2 of the acetylcholine receptor protein [36,221]. In large protein channels, however, transmembrane peptide sequences predominantly interact with other amino acids, a situation that is not well represented by the pure lipid matrix of the NMR samples.

Previous experiments indicate that the antibiotic activities of amphipathic model peptides are not correlated with the transmembrane orientations of helices [156]. Other models which have been suggested for antibiotic activity and pore formation are, therefore, presented below.

3.2. Wormhole model

Whereas the formation of transmembrane helical bundles seems a reasonable model to explain the well-defined step-wise conductivity increases observed for predominantly hydrophobic peptide sequences, such an arrangement results in the accumulation of many lysine and arginine residues in a highly restricted volume when bundles form of cationic peptides. In the case of a magainin hexamer, for example, 30 lysines would accumulate within a narrow pore of a few Ångstroms in diameter and ca. 30 Å in length [6]. In addition, the cation selectivity of pores formed by these latter peptides in the presence of PE/PS 1:1 membranes [105] seems to contrast the high positive charge density of the peptides. The transmembrane helical bundle model has, therefore, been modified, such that lipid together with peptides line the walls of toroidal openings [222,223]. At high peptide concentrations (>3.3 mol% corresponding to >10 wt.%), neutron in-plane scattering experiments on mechanically aligned membrane systems indeed indicate that water-filled cavities are present in the samples (named 'wormholes', Fig. 3B) [222]. However, the interpretation of such observations is difficult as the mosaic spread of the lipid and the peptide components in oriented samples increases at magainin concentrations >3 mol% (Bechinger, unpublished results). Moreover macroscopic phase transitions that correlate with alterations in peptide–lipid interactions have been observed at magainin-to-lipid ratios ≥ 3 mol% [133,135,224,225]. Further increases in peptide concentration result in the visible disintegration of the bilayers, probably into bicelles [92,163]. Although the formation of wormholes has been suggested to be an intermediate step during membrane micellisation and the development of antimicrobial activities, the experimental conditions of the neutron scattering experiments probably do not reflect the real situation in which channel-formation is observed in electrophysiological studies [105,107,108].

3.3. Carpet model

Models involving transmembrane orientations of amphipathic peptides are difficult to reconcile with observations that designed amphipathic helices (8–22 residues) show their strongest antibiotic activity when they consist of only 11–15 leucines and lysines [157]. The peptides with maximal antibiotic activities are, therefore, too short to cross the membrane. This observation is in agreement with solid-state NMR and IR spectroscopic investigations which indicate that these and related peptides are oriented parallel to the membrane surface [163,226]. Furthermore, the model peptide LAH_4 (cf. *supra*) exhibits much higher antibiotic activity at low pH, when oriented parallel to the membrane surface, than at neutral pH where the peptides adopt a transmembrane alignment [156].

Based on experimental results observed with the peptide antibiotic dermaseptin, a third model has been proposed [227]. This 34-residue peptide is rich in lysines and can be configured into an amphipathic α-helix (residues 1–27), thereby resembling cecropins and magainins. The peptide partitions into acidic and zwitterionic membranes; association with neutral membranes, however, happens with an apparent partition coefficient reduced by one order of magnitude [227]. It has been suggested that in the presence of negatively charged lipids and at high peptide concentrations, dermaseptin is located at the membrane surface and self-associates in a 'carpet-like' manner (Fig.

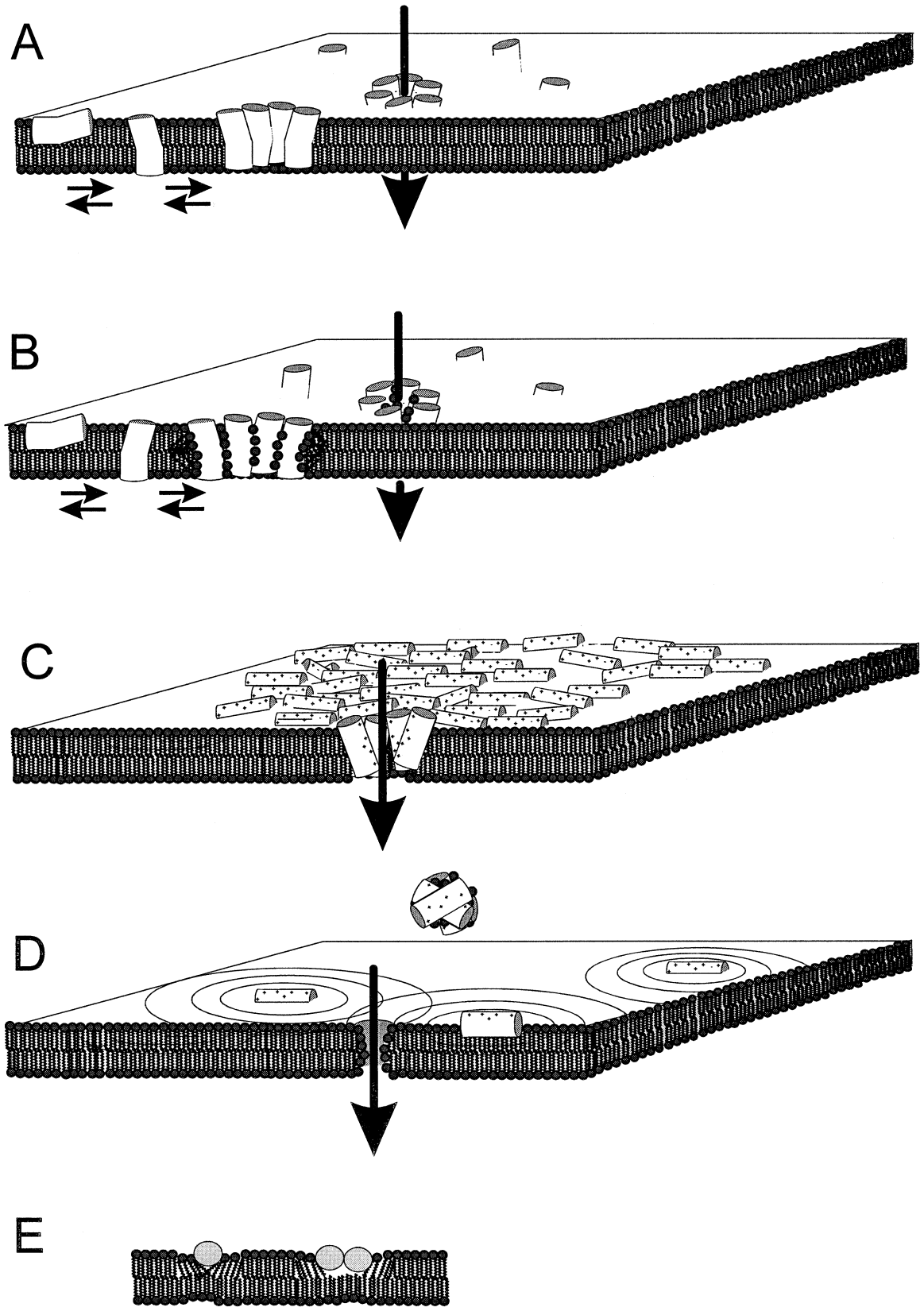
A
B
C
D
E

Fig. 3. Models for the occurrence of increases in conductivity across phospholipid membranes ('pore formation'). See text for details. (A) Transmembrane helical bundle of mostly hydrophobic polypeptides. (B) Wormhole model. (C) Carpet model. (D) In-plane diffusion model: peptide monomers are surrounded by areas of bilayer with irregular lipid packing characteristics. These diffuse along the surface of the bilayer causing transient openings when zones of metastability overlap. Alternatively, the detergent-like action of amphipathic peptides leads to the formation of peptide–lipid micelles, bilayer openings and the transient formation of pores. (E) The disruption of the lipid bilayer packing due to in-plane inserted peptides is schematically illustrated for monomers and side-to-side dimers. ←

3C). This model further suggests that the membrane breaks into pieces when a threshold concentration of peptide is reached [10]. At an intermediate stage wormhole formation has been suggested to occur [10]. Transmembrane pore formation may be possible, but according to the authors of this model, is not likely [227]. The presence of negatively charged lipids is important for a peptide carpet to form, as they help to reduce the repulsive electrostatic forces between positively charged peptides. In addition, high local peptide concentrations are achieved when cationic peptides phase-separate into domains rich in acidic phospholipids [138,228,229].

3.4. Detergent-like effects

The cytotoxic activity exhibited by cationic amphiphiles is most simply explained by taking into consideration their bilayer-disruptive properties. Disintegration of the bilayer results in the loss of the membrane barrier, dissipation of the transmembrane electrochemical gradient, loss of cytoplasmic constituents and interference with the energy metabolism of living cells (Fig. 3D). In a similar manner, the release of fluorescence dyes from model systems is probably a consequence of the peptide-induced disintegration of vesicular membranes. The onset of fluorescence dye leakage takes place at magainin concentrations of approximately 3 mol% which is equivalent to 81 g/mol lipid, a based-on-weight-value very similar to those observed for the permeability increases in the presence of the detergents Triton-X100 and octyl glucoside [114,230]. The initial asymmetric association at the outer surface of the vesicle only results in an enhancement of peptide-induced membrane instabilities and biphasic fluorophore release kinetics [114,231]. ^{31}P solid-state NMR spectroscopy indicates that addition of 2 mol% magainin to phosphatidylcholine bilayers results in the formation of an additional isotropic phase [163]. Further increasing the magainin 2 concentration leads to the clearance of the magainin phospholipid suspension and the appearance of phospholipid bilayers that are oriented with their membrane normal perpendicular to the magnetic field [92,163]. Similarly, addition of lysolipids [232] or detergents [233] result in the disintegration of phospholipid bilayers as well as magnetic orientation of bicelles [49]. In these latter structures a patch of bilayer is stabilised by a rim of short-chain lipids or detergents. Membrane disruptive properties have also been observed for other amphipathic helical peptides such as melittin [173,234], apolipoproteins [235], myelin basic protein [236], glucagon [237], signal sequences [238,239], and basic amphiphilic model peptides [240]. Micellar structures can either bud from the membrane at regions of high local peptide density [10] (Fig. 3C) or when small pre-formed peptide aggregates interact with lipid membranes [156,163,241] (Fig. 3D).

On a molecular level the intercalation of peptides between the phospholipid head groups corresponds to insertion of a cone-shaped molecule into the membrane (Fig. 3E). The head group of phosphatidylethanolamine occupies a smaller surface area in the interfacial region, therefore, this lipid corresponds to an inverted cone and more easily compensates for the strain imposed on the bilayer by inserted peptides [115,242] (Bechinger, unpublished results). Antibiotic action due to the membrane-lytic properties of in-plane oriented amphipathic peptide helices have been discussed at previous occasions [10,92,99,117, 118,156,243,44]. The observation of step-wise conductivity increases is, however, more difficult to explain [4,6].

3.5. In-plane diffusion model

Whereas the formation of carpet-like aggregates or the detergent-like disintegration of membranes deserves consideration when high local concentrations

of membrane-associated cationic peptides are present, comparatively low peptide-to-lipid ratios are needed to dissipate the ionic gradient across cell membranes or to develop antibiotic activity [10,99,100,242]. A model has therefore been proposed where lipid-mediated channel formation is based on the curvature strain imposed on lipid membranes in the presence of intercalated amphipathic peptides. This model is independent of cationic peptide aggregation, which is entropically and electrostatically disfavoured even in the presence of negatively charged phospholipids [6].

The diameter of a peptide helix is only about 12 Å, and therefore insufficient to span a lipid monolayer (Fig. 3E). Fluorescence energy transfer measurements indicate that the hydrophobic region of magainin 2 analogues, where phenylalanines have been replaced by tryptophans, is located approximately 10 Å from the bilayer centre [134]. The insertion of in-plane peptides into lipid bilayers, therefore, leads to disturbances in the bilayer packing within a diameter of approximately 100 Å and a reduction in the average bilayer thickness [225,245]. Diffusion of the peptides within the membrane causes regions of instability to overlap, disturbances of the lipid packing to accumulate, and transient openings to occur [6] (Fig. 3D). This latter model is in agreement with experimental findings including the non-cooperative membrane association of monomeric cecropins [99,117,141,246], the lack of peptide association within PG membranes which has been observed for magainin 2 at concentrations $\leq$5 mol% [247], the small co-operativity observed for magainins and cecropins in functional assays including channel formation [105,110,111,130,228,272], the in-plane orientation of amphipathic peptides [29,31,78,134,156], as well as translocation of lipid and peptide through bilayer openings or by diffusion along the lipid surface [231,248]. In addition, cecropin and magainin openings are in marked contrast to the pores formed by alamethicin (cf. *supra*). These former peptides show weak ion selectivity, variability of the conductance increases over three orders of magnitude, and the fluctuations within each conductivity level [104,105,108]. In addition, the permeability changes in the presence of magainins are rare and difficult to reproduce, as would be expected for a model based on molecular fluctuations [105,107,108].

Support for such a model is further derived from the observation that short peptides such as mastoparan (14 residues) [249], cecropin-melittin hybrids, some as short as 15 amino acids [250], and synthetic peptides (8–14 residues) [251–253] are also capable of exhibiting channel-like activity, although these peptide are too short to reach through the membrane. Furthermore, the charged amphipathic peptide sequence S4 from the sodium channel proteins, exhibits three conductance states at 70 pS, 300 pS and 500 pS when added to zwitterionic or mixed PC/PS membranes [254]. Interestingly, the first conductance level is permanently open and, therefore, correlated to the low-energy configurations also observed by structural methods. S4 exhibits α-helical secondary structures of 12 amino acids in length in membrane-like environments [29,255]. This helix orients parallel to the membrane interface as determined by proton-decoupled ^{15}N solid-state NMR spectroscopy in lipid bilayers, attenuation of NMR signal intensities by micelle-associated nitroxide radicals, or molecular modelling in a tetrachloromethane/water two-phase environment [29]. The average distance between chromophore-labelled S4 monomers or their location within the membrane is unaffected by transmembrane diffusion potentials [228].

Step-wise conductivity increases have also been observed in the presence of detergents [230,256], pure lipid membranes [257–259], or small unilamellar phospholipid vesicles when added to planar lipid bilayers [260], suggesting that an amphipathic distribution of charges and hydrophobic functional groups can be sufficient for the observation of channel-like events.

4. Regulation of antibiotic and channel activity

Regulation of selectivity and activities by peptide antibiotics can occur at any stage during the multistep process of accession to the membrane, bilayer association, insertion and pore formation: water soluble $\leftrightarrow$ surface accessible $\leftrightarrow$ surface associated $\leftrightarrow$ bilayer inserted $\leftrightarrow$ ... $\leftrightarrow$ openings.

In order to develop cytolytic activity, the peptide has to 'survive' exposure to serum or other media, and pass different barriers such as the extracellular matrix, or the bacterial lipopolysaccharides, outer

membrane and/or peptidoglycan layers [80]. Once it reaches the cell membrane its structures and topologies are in dynamic interchange [261,262]. The membrane association and cell-killing properties of cationic peptide amphiphiles are regulated by electrostatic and hydrophobic interactions which affect these multiple equilibria. Whereas the surface charge density of lipid bilayers has been shown to be of major importance for peptide association, the transmembrane potential seems to have a much smaller effect on membrane lysis. If electrostatic interactions are neglectable, such as in the outer leaflet of erythrocyte membranes, hydrophobic interactions become important. Biophysical investigations of these interactions are described in more detail below.

It has been shown that the presence of negatively charged lipids increases the local concentration of cationic peptides close to the membrane surface and therefore also their apparent association constants [99,130,263]. Whereas the outer monolayers of bacterial plasma membranes are rich in negative phospholipids, the membranes of healthy vertebrate cells appear neutral. Tumour cells, on the other hand, have lost part of their lipid asymmetry and therefore exhibit a more anionic character at their exterior [264]. The many like-charges of the peptides, however, also result in strong repulsive interactions. This has a twofold effect: first, the charges of the peptide screen the negative surface charge density of the lipid, therefore, the electrostatic contribution to the binding isotherm is strongly dependent on the amount of bound peptide and saturates at apparent charge equality [25]; second, electrostatic repulsion reduces the probability and life-time of peptide aggregates [265]. As these interactions are long range, the close approach of peptides and the formation of aggregates may even be suppressed completely [6].

Electrostatic interactions also arise from the presence of large inside-negative transmembrane potentials present in respiring procaryotic cells but not in erythrocytes [266]. It has been suggested that transmembrane electric potentials affect the partitioning of polypeptides between the aqueous and the lipid phase [220], the orientations of peptides within membranes [193], and the peptide bilayer penetration depth and polypeptide conformation [29].

Due to the composition of the outer leaflet of red cell membranes and the negligible transmembrane electric potential, electrostatic contributions are small [157,266]. Association and membrane-lytic activities of cationic amphiphiles are, therefore, governed by hydrophobic interactions. These are functions of the hydrophobic angle, the hydrophobic moment and the overall hydrophobicity of the peptides [158,242,267]. Reduction of the hydrophobicity of cecropin–magainin peptides correlates with decreases in haemolytic, but not antibiotic or fungicidal activities [140,157]. It has been shown that a large hydrophobic angle of magainin-derived model peptides increases the membrane permeabilising activity of the bound fraction as well as the ratio of antibacterial over haemolytic activities when keeping the hydrophobicity and the hydrophobic moment constant. [242].

Cholesterol, which is only present in eucaryotic cells, changes the interactions of cationic peptides with the membrane. It was shown, for example, that the incorporation of cholesterol into unilamellar vesicles of *Escherichia coli* phospholipid decreases the release of trapped glucose by cecropin analogues [268]. The cecropin-related conductivity across phospholipid membranes is also reduced due to the presence of cholesterol [104]. Cholesterol affects the fluidity and the dipole potential of phospholipid membranes and therefore modulates the activity of membrane-inserted peptides. In addition, the formation of hydrogen bonds between glutamates and cholesterol has been suggested to reduce antibiotic activity [269]. Interestingly, cholesterol delays the cell lytic effects of cecropins without abolishing them, suggesting that the peptide inserts more slowly into cholesterol-containing membranes [99,101]. A slowing of the insertion process or a modulated association behaviour might allow proteases to remove the toxins from the cellular surface [80,85,99,270].

Once inserted into the membrane, the peptide–lipid interactions, the composition of the phospholipid head groups and the fatty acyl chains all provide further levers for regulating channel and antibiotic activities when lipid-mediated models apply. Melittin, for example, has been shown to exhibit a rich variety of peptide–lipid interactions (cf. *supra*). The ability of amphipathic peptides to penetrate or to disrupt the membrane are dependent on the charge and the size of the lipid head group [156,242]. Although acidic lipids increase the membrane association of cationic peptides when taking

into account the amount of membrane-bound peptide only, it becomes obvious that the presence of PG lipids exerts a deactivating effect on their permeabilising properties [156,242]. This indicates significant differences in their interaction mechanisms. In addition, the inherent curvature of bilayer phospholipids may compensate or enhance the tendency for the formation of non-bilayer structures [115,242]. This is particularly true when the diffusion-controlled formation of bilayer defects is the underlying mechanism (Fig. 3D). Comparing the effects of magainin 2 on membranes with different phospholipid composition suggests these peptides impose positive curvature strain in zwitterionic membranes [115,163,242].

Additional regulatory pathways arise from the synergistic enhancements of antibiotic activities in naturally occurring cocktails of peptide antibiotics [10,93]. At 4 mol% total peptide concentration, the analysis of membrane-association isotherms suggests the formation of a stoichiometric 1:1 complex of PGLa and magainin 2 [94]. It is interesting to note that dimerised melittin allows fluorescence dye efflux from PC SUV to occur at increased rates when compared to monomeric melittin [271]. The authors of this latter study suggest a bilayer perturbation model similar to the one in Fig. 3D,E. Whereas the effects of a monomeric in-plane helix on the membrane are buffered by the surrounding lipids, a side-by-side intercalated dimer occupies twice the area on the membrane surface without a concomitant increase of the number of surrounding lipids (circumference). Filling the dimer induced defects by the lipids is, therefore, considerably more difficult. A similar model can explain the synergistic activity of combinations of other amphipathic peptides [10,93,118].

5. Conclusions

The interactions of amphipathic peptide antibiotics with lipid bilayers are characterised by a variety of reversible equilibria. The interaction contributions are electrostatic, hydrophobic, van der Waals and entropic in nature. The Gibbs free energies that describe these equilibria are usually composites of large quantities of opposite sign, and with our present knowledge difficult to assess in a quantitative manner. Matters are further complicated as lipid membranes are soft and capable of altering their geometrical features and macroscopic phase preferences in the presence of peptides. Nevertheless, a limited number of models, some of which relate to each other, have been suggested to explain the macroscopic structures of linear amphipathic peptides in membranes. In fact, the same peptide might interact with phospholipid membranes in different manners depending on the peptide-to-lipid ratio, the lipid composition of the membrane, the presence of salt and other experimental details. With the help of biophysical methods such as solid-state NMR spectroscopy, the conformation, topology and dynamics of membrane-associated peptides and lipids have been investigated in considerable detail. These techniques, therefore, have provided a wealth of structural data which allow a better understanding of the interactions underlying antibiotic activity and pore formation. These results have subsequently been used for the design of better and cheaper pharmaceuticals.

Acknowledgements

I am grateful to my co-workers, collaborators and colleagues who have contributed many results and ideas presented in this article. Martin Grimme, Gabriele Weingärtner and Kathrin Wieshuber have provided considerable help in managing the many references that have found their way into this review article. The contribution of Michael Helmle in simulating NMR spectra is gratefully acknowledged. Felicity Strang-Bechinger provided valuable support during proof-reading and discussing the manuscript.

References

[1] C.L. Bevins, M. Zasloff, Annu. Rev. Biochem. 59 (1990) 395–441.
[2] H.G. Boman, Cell 65 (1991) 205–207.
[3] P. Nicolas, A. Mor, Annu. Rev. Microbiol. 49 (1995) 277–304.
[4] R.E.W. Hancock, T. Falla, M. Brown, Adv. Microbiol. Physiol. 37 (1995) 135–175.
[5] G. Saberwal, N. Nagaraj, Biochim. Biophys. Acta 1197 (1994) 109–131.
[6] B. Bechinger, J. Membr. Biol. 156 (1997) 197–211.
[7] P.M. Hwang, H.J. Vogel, Biochem. Cell Biol. 76 (1998) 235–246.

[8] C.E. Dempsey, Biochim. Biophys. Acta 1031 (1990) 143–161.
[9] K. Lohner, R. Epand, Adv. Biophys. Chem. 6 (1997) 53–66.
[10] Z. Oren, Y. Shai, Biopolymers 47 (1998) 451–463.
[11] W.F. DeGrado, G.F. Musso, M. Lieber, E.T. Kaiser, F.J. Kezdy, Biophys. J. 37 (1982) 329–338.
[12] M.T. Tosteson, S.J. Holmes, M. Razin, D.C. Tosteson, J. Membr. Biol. 87 (1985) 35–44.
[13] D. Wade, A. Boman, B. Wahlin, C.M. Drain, D. Andreu, H.G. Boman, R.B. Merrifield, Proc. Natl. Acad. Sci. USA 87 (1990) 4761–4765.
[14] W.L. Maloy, U.P. Kari, Biopolymers 37 (1995) 105–122.
[15] B.A. Wallace, J. Struct. Biol. 121 (1998) 123–141.
[16] T.C. Terwilliger, L. Weissman, D. Eisenberg, Biophys. J. 37 (1982) 353–361.
[17] R. Bazzo, M.J. Tappin, A. Pastore, T.S. Harvey, J.A. Carver, I.D. Campbell, Eur. J. Biochem. 173 (1988) 139–146.
[18] C.E. Dempsey, Biochemistry 27 (1988) 6893–6901.
[19] L.R. Brown, W. Braun, A. Kumar, K. Wüthrich, Biophys. J. 37 (1982) 319–328.
[20] T. Ikura, N. Go, F. Inagaki, Proteins 9 (1991) 81–89.
[21] C.E. Dempsey, G.S. Butler, Biochemistry 31 (1992) 11973–11977.
[22] A. Okada, K. Wakamatsu, T. Miyazawa, T. Higashijima, Biochemistry 33 (1994) 9438–9446.
[23] B. Bechinger, J. Mol. Biol. 263 (1996) 768–775.
[24] E.J. Dufourc, I.C. Smith, J. Dufourcq, Biochemistry 25 (1986) 6448–6455.
[25] E. Kuchinka, J. Seelig, Biochemistry 28 (1989) 4216–4221.
[26] B. Bechinger, M. Zasloff, S.J. Opella, Biophys. J. 62 (1992) 12–14.
[27] F.D. Sonnichsen, J.E. Van Eyk, R.S. Hodges, B.D. Sykes, Biochemistry 31 (1992) 8790–8798.
[28] B. Bechinger, Proteins 27 (1997) 481–492.
[29] K. Mattila, R. Kinder, B. Bechinger, Biophys. J. 77 (1999) 2102–2113.
[30] J. Gesell, M. Zasloff, S.J. Opella, J. Biomol. NMR 9 (1997) 127–135.
[31] B. Bechinger, M. Zasloff, S.J. Opella, Biophys. J. 74 (1998) 981–987.
[32] M. Mehring, Principles of High Resolution NMR in Solids, Springer, Berlin, 1983.
[33] C.J. Hartzell, M. Whitfield, T.G. Oas, G.P. Drobny, J. Am. Chem. Soc. 109 (1987) 5966–5969.
[34] T.G. Oas, C.J. Hartzell, F.W. Dahlquist, G.P. Drobny, J. Am. Chem. Soc. 109 (1987) 5962–5966.
[35] N.D. Lazo, W. Hu, T.A. Cross, J. Magn. Res. 107 (1995) 43–50.
[36] B. Bechinger, Y. Kim, L.E. Chirlian, J. Gesell, J.-M. Neumann, M. Montal, J. Tomich, M. Zasloff, S.J. Opella, J. Biomol. NMR 1 (1991) 167–173.
[37] B. Bechinger, L.M. Gierasch, M. Montal, M. Zasloff, S.J. Opella, Solid State NMR 7 (1996) 185–192.
[38] F.A. Kovacs, T.A. Cross, Biophys. J. 73 (1997) 2511–2517.
[39] V. Wray, R. Kinder, T. Federau, P. Henklein, B. Bechinger, U. Schubert, Biochemistry 38 (1999) 5272–5282.
[40] A. Shoji, T. Ozaki, T. Fujito, K. Deguchi, S. Ando, I. Ando, Macromolecules 22 (1989) 2860–2863.
[41] A. Shoji, T. Ozaki, T. Fujito, K. Deguchi, S. Ando, I. Ando, J. Am. Chem. Soc. 112 (1990) 4693–4697.
[42] Q. Teng, T.A. Cross, J. Magn. Reson. 85 (1989) 439–447.
[43] I. Ando, T. Kameda, N. Asakawa, S. Kuroki, H. Kurosu, J. Mol. Struct. 441 (1998) 213–230.
[44] S.O. Smith, K. Aschheim, M. Groesbeek, Q. Rev. Biophys. 29 (1996) 395–449.
[45] L.M. McDowell, J. Schaefer, Curr. Opin. Struct. Biol. 6 (1996) 624–629.
[46] R.G. Griffin, Nat. Struct. Biol. NMR Suppl. (1998) 508–512.
[47] R.R. Ketchem, W. Hu, F. Tian, T.A. Cross, Structure 2 (1994) 699–701.
[48] J.J. de Vries, H.J.C. Berendsen, Nature 221 (1969) 1139–1140.
[49] C.R. Sanders II, J.H. Prestegard, Biophys. J. 58 (1990) 447–460.
[50] J.H. Prestegard, Nat. Struct. Biol. NMR Suppl. (1998) 517–522.
[51] C.R. Sanders, R.S. Prosser, Structure 6 (1998) 1227–1234.
[52] F. Ryan, The Forgotten Plague, Little Brown and Co., Boston, 1992.
[53] G.A. Woolley, B.A. Wallace, J. Membr. Biol. 129 (1992) 109–136.
[54] R.R. Ketchem, K.-C. Lee, S. Huo, T.A. Cross, J. Biomol. NMR 8 (1996) 1–14.
[55] T.A. Cross, Methods Enzymol. 289 (1997) 672–696.
[56] R. Smith, D.E. Thomas, F. Separovic, A.R. Atkins, B.A. Cornell, Biophys. J. 56 (1989) 307–314.
[57] R.S. Prosser, J.H. Davis, F.W. Dahlquist, M.A. Lindorfer, Biochemistry 30 (1991) 4687–4696.
[58] R.S. Prosser, S.I. Daleman, J.H. Davis, Biophys. J. 66 (1994) 1415–1428.
[59] A.W. Hing, S.P. Adams, D.F. Silbert, R.E. Norberg, Biochemistry 29 (1990) 4144–4156.
[60] W. Mai, W. Hu, C. Wang, T.A. Cross, Protein Sci. 2 (1993) 532–542.
[61] J.A. Killian, M.J. Taylor, R.E. Koeppe, Biochemistry 31 (1992) 11283–11290.
[62] K.C. Lee, S. Huo, T.A. Cross, Biochemistry 34 (1995) 857–867.
[63] F. Separovic, J. Gehrmann, T. Milne, B.A. Cornell, S.Y. Lin, R. Smith, Biophys. J. 67 (1994) 1495–1500.
[64] W. Hu, N.D. Lazo, T.A. Cross, Biochemistry 34 (1995) 14138–14146.
[65] R. Smith, D.E. Thomas, A.R. Atkins, F. Separovic, B.A. Cornell, Biochim. Biophys. Acta 1026 (1990) 161–166.
[66] F. Tian, T.A. Cross, J. Mol. Biol. 285 (1999) 1993–2003.
[67] B. Roux, M. Karplus, Biophys. J. 59 (1991) 961–981.
[68] D.A. Doyle, J.M. Cabral, R.A. Pfuetzner, A.L. Kuo, J.M. Gulbis, S.L. Cohen, B.T. Chait, R. MacKinnon, Science 280 (1998) 69–77.
[69] J.H. Davis, Biochemistry 27 (1988) 428–436.
[70] P.M. Macdonald, J. Seelig, Biochemistry 27 (1988) 2357–2364.

[71] A.W. Hing, S.P. Adams, D.F. Silbert, R.E. Norberg, Biochemistry 29 (1990) 4156–4166.
[72] K.C. Lee, W. Hu, T.A. Cross, Biophys. J. 65 (1993) 1162–1167.
[73] M. Bloom, Biophys. J. 69 (1995) 1631–1632.
[74] C.L. North, T.A. Cross, Biochemistry 34 (1995) 5883–5895.
[75] R.E. Koeppe, J.A. Killian, D.V. Greathouse, Biophys. J. 66 (1994) 14–24.
[76] W. Hu, T.A. Cross, Biochemistry 34 (1995) 14147–14155.
[77] D.D. Busath, C.D. Thulin, R.W. Hendershot, L.R. Phillips, P. Maughan, C.D. Cole, N.C. Bingham, S. Morrison, L.C. Baird, R.J. Hendershot, M. Cotten, T.A. Cross, Biophys. J. 75 (1998) 2830–2844.
[78] B. Bechinger, M. Zasloff, S.J. Opella, Protein Sci. 2 (1993) 2077–2084.
[79] R.E.W. Hancock, R. Lehrer, TIBTECH 16 (1998) 82–88.
[80] D. Andreu, L. Rivas, Biopolymers 47 (1999) 415–433.
[81] F. Garcia-Olmedo, A. Molina, J.M. Alamillo, P. Rodriguez-Palenzuela, Biopolymers 47 (1999) 479–491.
[82] R.A. Cruciani, J.L. Barker, M. Zasloff, H. Chen, O. Colamonici, Proc. Natl. Acad. Sci. USA 88 (1991) 3792–3796.
[83] Y. Ohsaki, A.F. Gazdar, H. Chen, B.E. Johnson, Cancer Res. 52 (1992) 3534–3538.
[84] H.M. Chen, W. Wang, D. Smith, S.C. Chan, Biochim. Biophys. Acta 1336 (1997) 171–179.
[85] A. Csordas, H. Michl, Monatshefte für Chemie 101 (1970) 182–189.
[86] W. Hoffmann, K. Richter, G. Kreil, EMBO J. 2 (1983) 711–714.
[87] B.W. Gibson, L. Poulter, D.H. Williams, J.E. Maggio, J. Biol. Chem. 261 (1986) 5341–5349.
[88] H. Steiner, D. Hultmark, A. Engstrom, H. Bennich, H.G. Boman, Nature 292 (1981) 246–248.
[89] D. Hultmark, A. Engstrom, H. Bennich, R. Kapur, H.G. Boman, Eur. J. Biochem. 127 (1982) 207–217.
[90] J.Y. Lee, A. Boman, C.X. Sun, M. Andersson, H. Jornvall, V. Mutt, H.G. Boman, Proc. Natl. Acad. Sci. USA 86 (1989) 9159–9162.
[91] H.G. Boman, B. Agerberth, A. Boman, Infect. Immun. 61 (1993) 2978–2984.
[92] R. Williams, R. Starmann, K.P. Taylor, K. Gable, T. Beeler, M. Zasloff, D. Covell, Biochemistry 29 (1990) 4490–4496.
[93] H.V. Westerhoff, M. Zasloff, J.L. Rosner, R.W. Hendler, A. de Waal, A. Vaz Gomes, P.M. Jongsma, A. Riethorst, D. Juretic, Eur. J. Biochem. 228 (1995) 257–264.
[94] K. Matsuzaki, Y. Mitani, K. Akada, O. Murase, S. Yoneyama, M. Zasloff, K. Miyajima, Biochemistry 37 (1998) 15144–15153.
[95] D. Andreu, M. Pons, J. Ubach, I. Fernandez, I.A. Boman, H.G. Boman, S.A. Mitchell, R.B. Merrifield, Peptides 1992 (1993) 763–765.
[96] S.Y. Shin, J.H. Kang, M.K. Lee, S.Y. Kim, Y.M. Kim, K.S. Hahm, Biochem. Mol. Biol. Int. 44 (1998) 1119–1126.
[97] H.V. Westerhoff, D. Juretic, R.W. Hendler, M. Zasloff, Proc. Natl. Acad. Sci. USA 86 (1989) 6597–6601.
[98] M. Hugosson, D. Andreu, H.G. Boman, E. Glaser, Eur. J. Biochem. 223 (1994) 1027–1033.
[99] L. Silvestro, K. Gupta, J.N. Weiser, P.H. Axelsen, Biochemistry 36 (1997) 11452–11460.
[100] D. Juretic, R.W. Hendler, F. Kamp, W.S. Caughey, M. Zasloff, H.V. Westerhoff, Biochemistry 33 (1994) 4562–4570.
[101] H. Steiner, D. Andreu, R.B. Merrifield, Biochim. Biophys. Acta 939 (1988) 260–266.
[102] R.B. Merrifield, E.L. Merrifield, P. Juvvadi, D. Andreu, H.G. Boman, Ciba Found. Symp. 186 (1994) 5–20.
[103] S. Vunnam, P. Juvvadi, K.S. Rotondi, R.B. Merrifield, Int. J. Peptide Protein Res. 51 (1998) 38–44.
[104] B. Christensen, J. Fink, R.B. Merrifield, D. Mauzerall, Proc. Natl. Acad. Sci. USA 85 (1988) 5072–5076.
[105] R.A. Cruciani, J.L. Barker, G. Raghunathan, H.R. Guy, M. Zasloff, E.F. Stanley, Eur. J. Pharmacol. 226 (1992) 287–296.
[106] H. Duclohier, Toxicology 87 (1994) 175–188.
[107] B. Haimovich, J.C. Tanaka, Biochim. Biophys. Acta 1240 (1995) 149–158.
[108] H. Duclohier, G. Molle, G. Spach, Biophys. J. 56 (1989) 1017–1021.
[109] S.R. Durell, G. Raghunathan, H.R. Guy, Biophys. J. 63 (1992) 1623–1631.
[110] A. Vaz Gomes, A. de Waal, J.A. Berden, H.V. Westerhoff, Biochemistry 32 (1993) 5365–5372.
[111] K. Matsuzaki, O. Murase, K. Miyajima, Biochemistry 34 (1995) 12553–12559.
[112] R.M. Epand, Y. Shai, J.P. Segrest, G.M. Anantharamaiah, Biopolymers 37 (1995) 319–338.
[113] G. Boheim, J. Membr. Biol. 19 (1974) 277–303.
[114] E. Grant, T.J. Beeler, K.M.P. Taylor, K. Gable, M.A. Roseman, Biochemistry 31 (1992) 9912–9918.
[115] K. Matsuzaki, K. Sugishita, N. Ishibe, M. Ueha, S. Nakata, K. Miyajima, R.M. Epand, Biochemistry 37 (1998) 11856–11863.
[116] J.H. Kang, S.Y. Shin, S.Y. Jang, M.K. Lee, K.-S. Hahm, J. Peptide Res. 52 (1998) 45–50.
[117] P. Diaz-Achirica, S. Prieto, J. Ubach, D. Andreu, E. Rial, L. Rivas, Eur. J. Biochem. 224 (1994) 257–263.
[118] C.L. Bashford, G.M. Alder, G. Menestrina, K.J. Micklem, J.J. Murphy, J.A. Pasternack, J. Biol. Chem. 261 (1986) 9300–9308.
[119] M.E. Houston, L.H. Kondejewski, D.N. Karunaratne, M. Gough, S. Fidai, R.S. Hodges, R.E.W. Hancock, J. Peptide Res. 52 (1998) 81–88.
[120] I. Fernandez, J. Ubach, F. Reig, D. Andreu, M. Pons, Biopolymers 34 (1994) 1251–1258.
[121] D.J. Hirsh, J. Hammer, W.L. Maloy, J. Blazyk, J. Schaefer, Biochemistry 35 (1996) 12733–12741.
[122] D. Andreu, R.B. Merrifield, H. Steiner, H.G. Boman, Biochemistry 24 (1985) 1683–1688.
[123] T.A. Holak, A. Engstrom, P.J. Kraulis, G. Lindeberg, H. Bennich, T.A. Jones, A.M. Gronenborn, G.M. Clore, Biochemistry 27 (1988) 7620–7629.

[124] D. Oh, S.J. Shin, J.H. Kang, K.-S. Hahm, K.L. Kim, Y. Kim, J. Peptide Res. 53 (1999) 578–589.
[125] H. Iwai, Y. Nakajima, S. Natori, Y. Arata, I. Shimada, Eur. J. Biochem. 271 (1993) 639–644.
[126] W. Xia, Q. Liu, J. Wu, Y. Xia, Y. Shi, X. Qu, Biochim. Biophys. Acta 1384 (1998) 299–305.
[127] L. Ragona, H. Molinari, L. Zetta, R. Longhi, D. Marchini, R. Dallai, L.F. Bernini, L. Lozzi, M. Scarselli, N. Niccolai, Biopolymers 39 (1996) 653–664.
[128] D. Sipos, M. Andersson, A. Ehrenberg, Eur. J. Biochem. 209 (1992) 163–169.
[129] A. Ramamoorthy, F.M. Marassi, M. Zasloff, S.J. Opella, J. Biomol. NMR 6 (1995) 329–334.
[130] K. Matsuzaki, M. Harada, S. Funakoshi, N. Fujii, K. Miyajima, Biochim. Biophys. Acta 1063 (1991) 162–170.
[131] A. Pines, M.G. Gibby, J.S. Waugh, J. Chem. Phys. 59 (1973) 569–590.
[132] B. Bechinger, J.M. Ruysschaert, E. Goormaghtigh, Biophys. J. 76 (1999) 552–563.
[133] S.J. Ludtke, K. He, Y. Wu, H.W. Huang, Biochim. Biophys. Acta 1190 (1994) 181–184.
[134] K. Matsuzaki, O. Murase, H. Tokuda, S. Funakoshi, N. Fujii, K. Miyajima, Biochemistry 33 (1994) 3342–3349.
[135] E. Jo, J. Blazyk, J.M. Boggs, Biochemistry 37 (1998) 13791–13799.
[136] M. Milik, J. Skolnick, Proteins 15 (1993) 10–25.
[137] R.G. Efremov, D.E. Nolde, G. Vergoten, A.S. Arseniev, Biophys. J. 76 (1999) 2460–2471.
[138] A. Latal, G. Degovics, R.F. Epand, R.M. Epand, K. Lohner, Eur. J. Biochem. 248 (1997) 938–946.
[139] T. Wieprecht, M. Dathe, M. Schürmann, E. Krause, M. Beyermann, M. Bienert, Biochemistry 35 (1996) 10844–10853.
[140] S.Y. Shin, J.H. Kang, K.S. Hahm, J. Peptide Res. 53 (1999) 82–90.
[141] E. Gazit, A. Boman, H.G. Boman, Y. Shai, Biochemistry 34 (1995) 11479–11488.
[142] E. Gazit, I.R. Miller, P.C. Biggin, M.S.P. Sansom, Y. Shai, J. Mol. Biol. 258 (1996) 860–870.
[143] L. Silvestro, P.H. Axelsen, Chem. Phys. Lipids 96 (1998) 69–80.
[144] J. Fink, A. Boman, H.G. Boman, R.B. Merrifield, Int. J. Peptide Protein Res. 33 (1989) 412–421.
[145] H. Michel, K.A. Weyer, H. Gruenberg, I. Dunger, D. Oesterhelt, F. Lottspeich, EMBO J. 5 (1986) 1149–1158.
[146] M. Chorev, M. Gurrath, V. Behar, S. Mammi, A. Tonello, E. Peggion, Biopolymers 36 (1995) 473–484.
[147] G.-S. Yi, C.B. Park, S.C. Kim, C. Cheong, FEBS Lett. 398 (1996) 87–90.
[148] H. Wong, J.H. Bowie, J.A. Carver, Eur. J. Biochem. 247 (1997) 545–557.
[149] A. Mor, V.H. Nguyen, A. Delfour, D. Migliore-Samour, P. Nicholas, Biochemistry 30 (1991) 8824–8830.
[150] H.J. Kim, S.K. Han, J.B. Park, H.J. Baek, B.J. Lee, P.D. Ryu, J. Peptide Res. 53 (1999) 1–7.
[151] T. Rozek, R.J. Waugh, S.T. Steinborner, J.H. Bowie, J.C. Wallace, M.J. Tyler, J. Peptide Sci. 4 (1998) 111–115.
[152] Y.G. Ge, D.L. MacDonald, K.J. Holroyd, C. Thornsberry, H. Wexler, M. Zasloff, Antimicrob. Agents Chemother. 43 (1999) 782–788.
[153] A. Tossi, M. Snocchi, M. Zanetti, P. Storici, R. Gennaro, Eur. J. Biochem. 228 (1995) 941–946.
[154] J. Boisbouvier, A. Prochnickachalufour, A.R. Nieto, J.A. Torres, N. Nanard, M.H. Rodriguez, L.D. Possani, M. Delepierre, Eur. J. Biochem. 257 (1998) 263–273.
[155] S.E. Blondelle, R.A. Houghten, TIBTECH 14 (1996) 60–65.
[156] T.C.B. Vogt, B. Bechinger, J. Biol. Chem. 274 (1999) 29115–29121.
[157] S.E. Blondelle, R.A. Houghten, Biochemistry 31 (1992) 12688–12694.
[158] T. Wieprecht, M. Dathe, E. Krause, M. Beyermann, W.L. Maloy, D.L. MacDonald, M. Bienert, FEBS Lett. 417 (1997) 135–140.
[159] R. Kinder, B. Bechinger, Biophys. J. (1999) A443.
[160] F. Jähnig, Proc. Natl. Acad. Sci. USA 80 (1983) 3691–3695.
[161] J.N. Israelachvilli, S. Marcelja, R.G. Horn, Q. Rev. Biophys. I3 (1980) 121–200.
[162] N. Numao, Y. Hirota, A. Iwahori, S. Kidokoro, M. Sasatsu, I. Kondo, S. Itoh, E. Itoh, T. Katoh, N. Shimozono, A. Yamazaki, K. Takao, S. Kobayashi, Biol. Pharmacol. Bull. 22 (1999) 73–76.
[163] B. Bechinger, R. Kinder, M. Helmle, T.B. Vogt, U. Harzer, S. Schinzel, Biopolymers 51 (1999) 174–190.
[164] T.C.B. Vogt, P. Ducarme, S. Schinzel, R. Brasseur, B. Bechinger, (1999) submitted.
[165] C. Altenbach, W. Froncisz, J.S. Hyde, W.L. Hubbell, Biophys. J. 56 (1989) 1183–1191.
[166] R. Smith, F. Separovic, T.J. Milne, A. Whittaker, F.M. Bennett, B.A. Cornell, A. Makriyannis, J. Mol. Biol. 241 (1994) 456–466.
[167] H. Vogel, Biochemistry 26 (1987) 4562–4572.
[168] S. Frey, L.K. Tamm, Biophys. J. 60 (1991) 922–930.
[169] J.P. Bradshaw, C.E. Dempsey, A. Watts, Mol. Membr. Biol. 11 (1994) 79–86.
[170] J. Seelig, P.M. Macdonald, P.G. Scherer, Biochemistry 26 (1987) 7535–7541.
[171] B. Bechinger, J. Seelig, Biochemistry 30 (1991) 3923–3929.
[172] G. Beschiaschvili, H.D. Baeuerle, Biochim. Biophys. Acta 1068 (1991) 195–200.
[173] J. Dufourcq, J.F. Faucon, G. Fourche, J.L. Dasseux, M. Le Maire, T. Gulik-Krzywicki, Biochim. Biophys. Acta 859 (1986) 33–48.
[174] C.E. Dempsey, A. Watts, Biochemistry 26 (1987) 5803–5811.
[175] C.R. Dawson, A.F. Drake, J. Helliwell, R.C. Hider, Biochim. Biophys. Acta 510 (1978) 75–86.
[176] J.F. Faucon, J.M. Bonmatin, J. Dufourcq, E.J. Dufourc, Biochim. Biophys. Acta 1234 (1995) 235–243.
[177] M. Monette, M.R. Van Calsteren, M. Lafleur, Biochim. Biophys. Acta 1149 (1993) 319–328.

[178] K.M. Sekharam, T.D. Bradrick, S. Georghiou, Biochim. Biophys. Acta 1063 (1991) 171–174.
[179] T. Pott, M. Paternostre, E.J. Dufourc, Eur. Biophys. J. 27 (1998) 237–245.
[180] T. Pott, E.J. Dufourc, Biophys. J. 68 (1995) 965–977.
[181] A.M. Batenburg, J.H. van Esch, B. De Kruijff, Biochemistry 27 (1988) 2324–2331.
[182] H. Vogel, F. Jähnig, Biophys. J. 50 (1986) 573–582.
[183] T. Maurer, C. Lucke, H. Ruterjans, Eur. J. Biochem. 196 (1991) 135–141.
[184] P. Yuan, P.J. Fisher, F.G. Prendergast, M.D. Kemple, Biophys. J. 70 (1996) 2223–2238.
[185] A.J. Weaver, M.D. Kemple, J.W. Brauner, R. Mendelsohn, F.G. Prendergast, Biochemistry 31 (1992) 1301–1313.
[186] A.M. Batenburg, J.C. Hibbeln, A.J. Verkleij, B. De Kruijff, Biochim. Biophys. Acta 903 (1987) 142–154.
[187] A.M. Batenburg, J.H. van Esch, J. Leunissen-Bijvelt, A.J. Verkleij, B. De Kruijff, FEBS Lett. 223 (1987) 148–154.
[188] A.M. Batenburg, J.C. Hibbeln, B. De Kruijff, Biochim. Biophys. Acta 903 (1987) 155–165.
[189] C. Dempsey, M. Bitbol, A. Watts, Biochemistry 28 (1989) 6590–6596.
[190] M. Lafleur, J.F. Faucon, J. Dufourcq, M. Pezolet, Biochim. Biophys. Acta 980 (1989) 85–92.
[191] S. Ohki, E. Marcus, D.K. Sukumaran, K. Arnold, Biochim. Biophys. Acta 1194 (1994) 223–232.
[192] M. Monette, M. Lafleur, Biophys. J. 68 (1995) 187–195.
[193] M.S. Sansom, Eur. Biophys. J. 22 (1993) 105–124.
[194] D.S. Cafiso, Annu. Rev. Biophys. Biomol. Struct. 23 (1994) 141–165.
[195] R.O. Fox Jr., F.M. Richards, Nature 300 (1982) 325–330.
[196] A.A. Yee, J.D. O'Neil, Biochemistry 31 (1992) 3135–3143.
[197] J.C. Franklin, J.F. Ellena, S. Jayasinghe, L.P. Kelsh, D.S. Cafiso, Biochemistry 33 (1994) 4036–4045.
[198] C.L. North, J.C. Franklin, R.G. Bryant, D.S. Cafiso, Biophys. J. 67 (1994) 1861–1866.
[199] D.P. Tieleman, M.S.P. Sansom, H.J.C. Berendsen, Biophys. J. 76 (1999) 40–49.
[200] J. Jacob, H. Duclohier, D.S. Cafiso, Biophys. J. 76 (1999) 1367–1376.
[201] S. Furois-Corbin, A. Pullman, Biochim. Biophys. Acta 944 (1988) 399–413.
[202] F. Fraternali, Biopolymers 30 (1990) 1083–1099.
[203] M. Cascio, B.A. Wallace, Proteins 4 (1988) 89–98.
[204] V. Brumfeld, I.R. Miller, Biochim. Biophys. Acta 1024 (1990) 49–53.
[205] W.T. Heller, K. He, S.J. Ludtke, T.A. Harroun, H.W. Huang, Biophys. J. 73 (1997) 239–244.
[206] C.L. North, M. Barranger-Mathys, D.S. Cafiso, Biophys. J. 69 (1995) 2392–2397.
[207] M. Barranger-Mathys, D.S. Cafiso, Biochemistry 35 (1996) 498–505.
[208] S. Jayasinghe, M. Barranger-Mathys, J.F. Ellena, C. Franklin, D.S. Cafiso, Biophys. J. 74 (1998) 3023–3030.
[209] R.J. Taylor, R. de Levie, Biophys. J. 59 (1991) 873–879.
[210] G. Schwarz, C.H. Robert, Biophys. J. 58 (1990) 577–583.
[211] M. Eisenberg, J.E. Hall, C.A. Mead, J. Membr. Biol. 14 (1973) 143–176.
[212] L.G. Gordon, D.A. Haydon, Biochim. Biophys. Acta 255 (1972) 1014–1018.
[213] W. Hanke, G. Boheim, Biochim. Biophys. Acta 596 (1980) 456–462.
[214] M.S.P. Sansom, in: D. Noble, T.L. Blundell (Eds.), Progress in Biophysics and Molecular Biology, Pergammon, Oxford, 1991, pp. 139–235.
[215] G. Boheim, H.-A. Kolb, J. Membr. Biol. 38 (1978) 99–150.
[216] G. Boheim, W. Hanke, G. Jung, Biophys. Struct. Mech. 9 (1983) 181–191.
[217] G.A. Woolley, R.M. Epand, I.D. Kerr, M.S. Sansom, B.A. Wallace, Biochemistry 33 (1994) 6850–6858.
[218] J. Breed, I.D. Kerr, R. Sankararamakrishnan, M.S. Sansom, Biopolymers 35 (1995) 639–655.
[219] G. Schwarz, P. Savko, Biophys. J. 39 (1982) 211–219.
[220] S. Stankowski, U.D. Schwarz, G. Schwarz, Biochim. Biophys. Acta 941 (1988) 11–18.
[221] S.J. Opella, F.M. Marassi, J.J. Gesell, A.P. Valente, Y. Kim, M. Oblatt-Montal, M. Montal, Nat. Struct. Biol. 6 (1999) 374–379.
[222] S.J. Ludtke, K. He, W.T. Heller, T.A. Harroun, L. Yang, H.W. Huang, Biochemistry 35 (1996) 13723–13728.
[223] K. Matsuzaki, Biochim. Biophys. Acta 1376 (1998) 391–400.
[224] M. Wenk, J. Seelig, Biochemistry 37 (1998) 3909–3916.
[225] C. Münster, Y. Lu, S. Schinzel, B. Bechinger, T. Salditt, Eur. Biophys. J. 28 (1999) in press.
[226] S. Castano, B. Desbat, M. Laguerre, J. Dufourq, Biochim. Biophys. Acta 1416 (1999) 176–194.
[227] Y. Pouny, D. Rapaport, A. Mor, P. Nicolas, Y. Shai, Biochemistry 31 (1992) 12416–12423.
[228] D. Rapaport, M. Danin, E. Gazit, Y. Shai, Biochemistry 31 (1992) 8868–8875.
[229] R. Welti, M. Glaser, Chem. Phys. Lipids 73 (1994) 121–137.
[230] P. Schlieper, E. De Robertis, Arch. Biochem. Biophys. 184 (1977) 204–208.
[231] K. Matsuzaki, O. Murase, N. Fujii, K. Miyajima, Biochemistry 34 (1995) 6521–6526.
[232] K. Inoue, K. Suzuki, S. Nojima, J. Biol. Chem. 81 (1977) 1097–1106.
[233] C.R. Sanders II, J.H. Prestegard, Biophys. J. 58 (1990) 447–460.
[234] C.E. Dempsey, B. Sternberg, Biochim. Biophys. Acta 1061 (1991) 175–184.
[235] J.P. Segrest, D.W. Garber, C.G. Brouillette, S.C. Harvey, G.M. Anantharamaiah, Adv. Protein Chem. 45 (1994) 303.
[236] M. Roux, F.A. Nezil, M. Monck, M. Bloom, Biochemistry 33 (1994) 307–311.
[237] A.J.S. Jones, R.M. Epand, K.F. Lin, D. Walton, W.J. Vail, Biochemistry 17 (1978) 2301–2307.
[238] A.M. Batenburg, R.A. Demel, A.J. Verkleij, B. De Kruijff, Biochemistry 27 (1988) 5678–5685.

[239] J.A. Killian, A.M. de Jong, J. Bijvelt, A.J. Verkleij, B. De Kruijff, EMBO J. 9 (1990) 815–819.
[240] J.A. Reynaud, J.P. Grivet, D. Sy, Y. Trudelle, Biochemistry 32 (1993) 4997–5008.
[241] J. Bello, H.R. Bello, E. Granados, Biochemistry 21 (1982) 461–465.
[242] T. Wieprecht, M. Dathe, R.M. Epand, M. Beyermann, E. Krause, W.L. Maloy, D.L. MacDonald, M. Bienert, Biochemistry 36 (1997) 12869–12880.
[243] J.P. Segrest, H. De Loof, J.G. Dohlmann, C.G. Brouillette, G.M. Anatharamaiah, Proteins 8 (1990) 103–117.
[244] E. Gazit, W.J. Lee, P.T. Brey, Y. Shai, Biochemistry 33 (1994) 10681–10692.
[245] S. Ludtke, K. He, H. Huang, Biochemistry 34 (1995) 16764–16769.
[246] H.S. Mchaourab, J.S. Hyde, J.B. Feix, Biochemistry 33 (1994) 6691–6699.
[247] M. Schumann, M. Dathe, T. Wieprecht, M. Beyermann, M. Bienert, Biochemistry 36 (1997) 4345–4351.
[248] K. Matsuzaki, O. Murase, N. Fujii, K. Miyajima, Biochemistry 35 (1996) 11361–11368.
[249] I.R. Mellor, M.S.P. Sansom, Proc. R. Soc. Lond. B 239 (1990) 383–400.
[250] E.L. Merrifield, S.A. Mitchell, J. Ubach, H.G. Boman, D. Andreu, R.B. Merrifield, Int. J. Peptide Protein Res. 46 (1995) 214–220.
[251] J.D. Lear, Z.R. Wasserman, W.F. DeGrado, Science 240 (1988) 1177–1181.
[252] K. Anzai, M. Hamasuna, H. Kadono, S. Lee, H. Ayoagi, Y. Kyrino, Biochim. Biophys. Acta 1064 (1991) 256–266.
[253] Y. Higashimoto, H. Kodama, M. Jelokhani-Niaraki, F. Kato, M. Kondo, J. Biochem. 125 (1999) 705–712.
[254] M.T. Tosteson, D.S. Auld, D.C. Tosteson, Proc. Natl. Acad. Sci. USA 86 (1989) 707–710.
[255] D.G. Doak, D. Mulvey, K. Kawaguchi, J. Villalain, I.D. Campbell, J. Mol. Biol. 258 (1996) 672–687.
[256] G.M. Alder, W.M. Arnold, C.L. Bashford, A.F. Drake, C.A. Pasternak, U. Zimmermann, Biochim. Biophys. Acta 1061 (1991) 111–120.
[257] V.F. Antonov, V.V. Petrov, A.A. Molnar, D.A. Predvoditelev, A.S. Ivanov, Nature 283 (1980) 585–586.
[258] K. Kaufmann, I. Silman, Biophys. Chem. 18 (1983) 89–99.
[259] K. Yoshikawa, T. Fujimoto, T. Shimooka, H. Terada, N. Kumazawa, T. Ishii, Biophys. Chem. 29 (1988) 293–299.
[260] D.J. Woodbury, J. Membr. Biol. 109 (1989) 145–150.
[261] S. Lambotte, P. Jasperse, B. Bechinger, Biochemistry 37 (1998) 16–22.
[262] M.S.P. Sansom, Curr. Opin. Colloid Interface Sci. 3 (1998) 518–524.
[263] G. Beschiaschvili, J. Seelig, Biochemistry 29 (1990) 52–58.
[264] T. Utsugi, A.J. Schroit, J. Connor, C.D. Bucana, I.J. Fidler, Cancer Res. 51 (1991) 3062–3066.
[265] K. Matsuzaki, A. Nakamura, O. Murase, K. Sugishita, N. Fujii, K. Miyajima, Biochemistry 36 (1997) 2104–2111.
[266] K. Matsuzaki, K. Sugishita, N. Fujii, K. Miyajima, Biochemistry 34 (1995) 3423–3429.
[267] E.M. Tytler, J.P. Segrest, R.M. Epand, S.Q. Nie, R.F. Epand, V.K. Mishna, Y.V. Venkatachalapathi, G.M. Anantharamaiah, J. Biol. Chem. 268 (1993) 22121.
[268] Y. Nakajima, X.-m. Qu, S. Natori, J. Biol. Chem. 262 (1987) 1665–1669.
[269] E.M. Tytler, G.M. Anantharamaiah, D.E. Walker, V.K. Mishra, M.N. Palgunachari, J.P. Segrest, Biochemistry 34 (1995) 4393–4401.
[270] N.M. Resnick, W.L. Maloy, H.R. Guy, M. Zasloff, Cell 66 (1991) 541–554.
[271] J. Takei, A. Remenyi, C.E. Dempsey, FEBS Lett. 442 (1999) 11–14.
[272] T. Wieprecht, M. Beyermann, J. Seelig, Biochemistry 38 (1999) 10377–10378.